Published in final edited form as:
Cell Signal. 2010 May ; 22(5): 809–820. doi:10.1016/j.cellsig.2010.01.005.

WNT1-Inducible Signaling Pathway Protein-1 Activates Diverse Cell Survival Pathways and Blocks Doxorubicin-induced Cardiomyocyte Death

Balachandar Venkatesan[1], **Sumanth D. Prabhu**[2], **Kaliyamurthi Venkatachalam**[3], **Srinivas Mummidi**[3], **Anthony J. Valente**[3], **Robert A. Clark**[3], **Patrice Delafontaine**[1], and **Bysani Chandrasekar**[1,4,*]

[1]Heart and Vascular Institute, Tulane University School of Medicine, New Orleans, LA 70112

[2]Institute of Molecular Cardiology, Department of Medicine, University of Louisville, Louisville, KY 40292, and the Medical Service, Louisville Veterans Affairs Medical Center, Louisville, KY 40206

[3]Department of Medicine, University of Texas Health Science Center, San Antonio, TX 78229

[4]Research Service, Southeast Louisiana Veterans Health Care System, New Orleans, LA 70161

Abstract

The anthracycline antibiotic doxorubicin (DOX) is a potent cancer chemotherapeutic agent that exerts both acute and chronic cardiotoxicity. Here we show that in adult mouse cardiomyocytes, DOX activates (i) the pro-apoptotic p53, (ii) p38MAPK and JNK, (iii) Bax translocation, (iv) cytochrome *c* release, and (v) caspase 3. Further, it (vi) inhibits expression of anti-apoptotic Akt, Bcl-2 and Bcl-xL, and (vii) induces internucleosomal degradation and cell death. WNT1-Inducible Signaling Pathway Protein-1 (WISP1), a CCN family member and a matricellular protein, inhibits DOX-mediated cardiomyocyte death. WISP1 inhibits DOX-induced p53 activation, p38 MAPK and JNK phosphorylation, Bax translocation to mitochondria, and cytochrome *c* release into cytoplasm. Additionally, WISP1 reverses DOX-induced suppression of Bcl-2 and Bcl-xL expression and Akt inhibition. The pro-survival effects of WISP1 were recapitulated by the forced expression of mutant p53, wild-type Bcl-2, wild-type Bcl-xL, or constitutively active Akt prior to DOX treatment. WISP1 also induces the pro-survival factor Survivin via PI3K/Akt signaling. Overexpression of wild-type, but not mutant Survivin, blunts DOX cytotoxicity. Further, WISP1 stimulates PI3K-Akt-dependent GSK3β phosphorylation and β-catenin nuclear translocation. Importantly, WISP1 induces its own expression. Together, these results provide important insights into the cytoprotective effects of WISP1 in cardiomyocytes, and suggest a potential therapeutic role for WISP1 in DOX-induced cardiotoxicity.

Keywords

CCN; WISP; doxorubicin; cardiomyocytes; growth factors; cardiotoxicity

*Correspondence to: Bysani Chandrasekar, DVM, Ph.D., Heart and Vascular Institute, Tulane University School of Medicine, 1430 Tulane Avenue, SL-48, New Orleans, LA 70112, Telephone: 504-988-3034, Fax: 504-988-4237, bchandra@tulane.edu.

1. Introduction

Doxorubicin (DOX) is an anthracycline antibiotic used widely in treating various malignancies in both children and adults [1;2;3;4]. However, it also causes acute and chronic cardiotoxicity, which limits its use. DOX is known to induce cardiomyocyte death, aberrant calcium signaling, myocardial contractile dysfunction, progressive cardiomyopathy, and congestive heart failure [1;3;4]. In cardiomyocytes, it activates oxidative stress-dependent and independent signaling pathways, intrinsic (mitochondrial) and extrinsic (cytoplasmic) pro-apoptotic signaling mechanisms, leading ultimately to cell death [4;5;6;7]. Its toxic effects are especially pronounced in fetal and neonatal cardiomyocytes, implying that its cardiotoxic effects are cumulative in children [3;4;5].

Following DOX treatment of cardiomyocytes in vitro and administration in vivo, DOX rapidly accumulates in the nucleus where it interferes with DNA stability. DOX damages DNA and activates p53-dependent signaling pathways [8;9]. DOX also accumulates in mitochondria [10], inducing mitochondrial injury and activating mitochondrial cell death pathways. Though p53 plays a critical role in DNA repair [11;12], paradoxically its activation also stimulates cell death. In fact, inhibition of p53 by pifithrin (PFT)-α, a cell-permeable p53 inhibitor [8;13], inhibits the pro-apoptotic effects of DOX in vitro, with similar survival effects reported in vivo in p53-disrupted mice [14], suggesting a critical role for p53 in DOX-induced cytotoxicity.

WNT1-Inducible Signaling Pathway Protein-1 (WISP1), a member of the CYR61/CTGF/Nov (CCN) family of growth factors, is a secreted matricellular protein. It is overexpressed in both cancer cell lines and human tumors [15;16]. Its forced expression results in transformation and proliferation of normal rat kidney fibroblast cells, and promotes tumor formation in nude mice [17]. It induces growth in cardiomyocytes, and stimulates proliferation of cardiac fibroblasts [18]. *In vivo*, WISP1 expression is increased following myocardial infarction, where it is localized predominantly to border and non-infarcted remote zones [18;19]. This suggests that WISP1 may play a role in the growth or hypertrophy of the post-infarct surviving cardiomyocytes. Thus WISP1 may act as a potent pro-survival factor that antagonizes cardiomyocyte death in response to various adverse and stress conditions.

WISP1 negatively regulates p53 activation. Su et al. reported that WISP1 activates the pro-survival Akt-dependent signaling pathway in normal rat kidney fibroblasts [20]. In human lung carcinoma cells, WISP1 over-expression antagonized apoptosis induced by UV irradiation, etoposide treatment, or γ-irradiation [20]. These agents induce DNA damage and promote cell death via activation of p53. Further, WISP1 over-expression in these cells resulted in Akt phosphorylation, upregulation of antiapoptotic Bcl-xL expression, and inhibition of mitochondrial release of cytochrome *c* [20]. Importantly, WISP1 also blocked cell death at a late stage in the p53-mediated apoptosis pathway [20]. However, WISP1 overexpression did not prevent Fas ligand-activated cell death, indicating that WISP1 acts in a stimulus-specific fashion, exerting its pro-survival effects via inhibiting p53 activation and p53-dependent signaling.

Since DOX activates p53 and induces cardiomyocyte death [8;9], and since WISP1 exerts potent pro-survival effects in both cardiomyocytes as well as other cells [17;18;19;20], we investigated whether WISP1 antagonizes DOX-mediated cardiomyocyte death, and determined the underlying mechanisms. Our results demonstrate for the first time that WISP1 significantly inhibits DOX-induced cardiomyocyte death via: (i) inhibition of p53 (ii) attenuation of both intrinsic and extrinsic cell death pathways, and (iii) activation of diverse cell survival pathways. These results provide important insights into the cytoprotective effects of WISP1 in cardiomyocytes, and suggest a potential therapeutic role for WISP1 in DOX-induced cardiotoxicity.

2. Materials and methods

2.1. Materials

Recombinant human WISP1 (rhWISP1 or WISP1) was purchased from PeproTech (Rocky Hill, NJ). PI3K inhibitors Ly294002 (25 μM in DMSO for 1 h) and wortmannin (250 nM in DMSO for 1 h), Akt inhibitor X (Akti-X, # 124040, 2.5 μM in water for 1 h), p38 MAPK inhibitor SB 203580 (1 μM in DMSO for 30 min), JNK inhibitor SP 600125 (20 μM in DMSO for 30 min), proteasomal inhibitor lactacystin (5 μM in DMSO for 30 min), and DMSO were purchased from EMD Biosciences (Gibbstown, NJ 08027). Akti-X is a cell-permeable selective inhibitor of Akt phosphorylation and kinase activity with minimal effect on PI3K, PDK1 and SGK1[21]. p53 inhibitor PFT-α (1-(4-methylphenyl)-2-(4,5,6,7-tetrahydro-2-imino-3(2H) benzothiazolyl)ethanone-hrdrobromide; 100 μM in DMSO for 2 h) and SB-216763 (3-(2,4-Dichlorophenyl)-4-(1-methyl-1H-indol-3yl)-1H-pyrrole-2,5-dione; 1 nM in DMSO for 15 min), a selective GSK3β inhibitor that blocks the GSK3β binding site for ATP were obtained from BIOMOL International (Plymouth Meeting, PA). LiCl (30 mM for 15 min) was used as a positive control for chemical inhibition of GSK3β [22]. At the indicated concentrations and for the duration of treatment, the pharmacological inhibitors of p53, PI3K, Akt, GSK3β and proteasome failed to modulate adherence to culture dishes, morphology, or viability of cardiomyocytes (data not shown). Enhanced chemiluminescence detection kit was from Amersham Pharmacia Biotech. All tissue culture supplies were from Invitrogen Corporation (Carlsbad, CA). Antibodies against p53, p38 MAPK (#9212), phospho p38 MAPK (p-p38 MAPK Thr180/Tyr182, #9211), Akt (#9272), pAkt (Thr308, #9275), GSK-3β (27C10; #9315), phospho-GSK-3β (Ser9, #9336), cleaved PARP (Asp214; #9544), Bax (#2772), Bcl-xL (#2762; recognizes only the long form and is used to detect Bcl-xL in mitochondrial fraction) and α-tubulin (#2144) were purchased from Cell Signaling Technology, Inc. (Beverly, MA). Antibody to Bcl-x that recognizes both long and short forms (B12017) was purchased from Stratagene (LaJolla, CA). PARP (sc-1562), JNK (sc-81468), pJNK (Thr183/Tyr185, sc-12882), WISP1 neutralizing antibodies (sc-25441), anti-PI3Kp85, and Survivin (sc-10811) antibodies were from Santa Cruz Biotechnology, Inc. Anti-glyceraldehyde-3-phosphate dehydrogenase (GAPDH; MAB374) and anti-mitochondrial protein β-subunit of complex V (V-β; A21351) antibodies were purchased from Millipore (Billerica, MA) and Invitrogen, respectively. The caspase-3 inhibitor Z-DEVD-fmk, pancaspase inhibitor Z-VAD-fmk, and the negative control Z-FA-fmkwere obtained from Enzyme Systems Products (Livermore, CA), and were used at 50 μM in DMSO. Doxorubicin (1 μM in water) and other biochemicals were purchased from Sigma-Aldrich.

2.2. Cell culture

All experiments were performed in male adult (12 weeks) C57Bl/6 mice (Charles River Laboratories). The investigation conformed to the Guide for the Care and Use of Laboratory Animals published by the US National Institutes of Health (NIH Publication No. 85-23, revised 1996) and was approved by the institutional animal care and use committee. Calcium-tolerant ventricular myocytes were isolated as we have described previously [18;19], using a modified Langendorff perfusion and collagenase digestion technique adapted from the methodology described by the Alliance for Cellular Signaling (http://www.signalinggateway.org). The cells were plated on 35-mm cell culture dishes precoated with 20 μg/ml mouse laminin in phosphate-buffered saline with 1% penicillin-streptomycin for 1 h. Cardiomyocytes were maintained under resting conditions in a humidified incubator for at least 16 h before experimentation. All the studies were completed within 72 h following isolation

2.3. Adenoviral transduction

Adenoviral vectors for dominant-negative (dn) PI3Kp85 (Ad.dnPI3K), dnAkt (Ad.dnAkt), constitutively active Akt (Ad.myr.Akt), GFP (Ad.GFP), and Ad.MCS-Luc have been

previously described [23;24]. Ad.Survivin and Ad.mSurvivin were kindly provided by Dario C. Altieri (Department of Cancer Biology and the Cancer Center, University of Massachusetts Medical School, Worcester, MA) [24]. Ad.Bcl-2, Ad.myr.Akt, Ad.mp53, Ad.p53-Luc, and Ad.pRL-Luc were purchased from Vector Biolabs (Philadelphia, PA). Ad.Bcl-xL was provided by A. Gambotto of the Vector Core Facility at the University of Pittsburgh (Pittsburgh, PA). Cardiomyocytes were infected at a multiplicity of infection (MOI) of 100 for 1 h at 22 °C in PBS. The infection medium was replaced with medium containing 0.5% BSA. After 24 h, cells were treated with rhWISP1. The transfection efficiency with adenoviral vectors was approximately 100% as determined by the expression of GFP in cardiomyocytes infected with Ad.GFP (data not shown). Infection with the adenoviral vectors had no detectable effect on cardiomyocyte morphology, viability and adherence.

2.4. p53 activation

Nuclear proteins were extracted using the Panomics Nuclear Extraction Kit (#AY2002; Affymetrix, Inc., Fremont, CA). Purity of nuclear extracts was confirmed by the presence of lamin and absence of GAPDH immunoreactivity. p53 protein-DNA complex formation was assessed by electrophoretic mobility shift assay (EMSA) using cardiomyocyte nuclear extracts and double-stranded consensus DNA for p53 (5'-TACAGAACATGTCTAAGCATGCTGGGG-3' (sc-2579). Mutant p53 (5'-TACAGAATCGCTCTAAGCATGCTGGGG-3' (sc-2580) served as a control (Santa Cruz Biotechnology, Inc.). Activation of p53 was confirmed by ELISA (TransAM TF ELISA kit, 43296 ; Active Motif, Carlsbad, CA). p53 activation was also analyzed by reporter assays using adenoviral transduction of a p53 reporter vector (Ad-p53-Luc, MOI 50) in which firefly luciferase expression is regulated by 14 direct repeats of the p53 transcription recognition sequence. Ad.MCS-Luc served as a control. Ad.pRL-Luc (MOI 50) served as an internal control. After incubation for the indicated time periods, the cells were harvested for the dual-luciferase assay. Data were normalized by dividing firefly luciferase activity by that of the corresponding *Renilla* luciferase.

2.5. Phosphatidylinositol 3-kinase

PI3 kinase activity was determined using a commercially available PI3-kinase ELISA kit (Echelon Biosciences Inc., Salt Lake City, UT) [23]. Cardiomyocytes were transduced with Ad.dnPI3Kp85 prior to DOX addition (1 μM for 1 h), washed in ice-cold PBS and lysed in 500 μl ice-cold lysis buffer [137 mM NaCl, 20 mM Tris-HCl (pH 7.4), 1 mM $CaCl_2$, 1 mM $MgCl_2$, 0.1 mM sodium orthovanadate, 1% NP-40 and 1 mM PMSF] before immunoprecipitation and assayed according to the manufacturer's instructions. The level of the PI3K component p85α was determined by immunoblotting.

2.6. Akt/Protein Kinase B (PKB)

Total and phospho-Akt (pAkt Thr308) levels in whole cell homogenates were analyzed by immunoblotting [18;19;23]. The immunoreactive bands were detected by chemiluminescence, and quantified by densitometry. Akt kinase activity was analyzed using an immunecomplex kinase assay (Cell Signaling Technology, Inc.) based on Akt-induced phosphorylation of glycogen synthase kinase-3 (GSK-3).

2.7. Caspase 3 activity

Caspase-3 activity was determined using a fluorescent method (EMD Chemicals, Gibbstown, NJ). The assay is based on cleavage downstream of aspartate residues in the peptide sequence DEVD labeled with a fluorescent molecule, 7-amino-4-trifluoromethyl coumarin. Cardiomyocytes were homogenized in the provided lysis buffer, and centrifuged at 10,000*g* for 20 min at 4°C. The resulting supernatant was used for protein estimation and caspase-3

activity assay. The cell lysates were treated with the substrate conjugate, and the resulting fluorescent intensity was measured in a fluorescent plate reader at excitation and emission wavelengths of 400 and 505 nm, respectively. The data are expressed as a percent increase from the untreated control values.

2.8. Cytochrome c release

DOX-mediated cardiomyocyte death was also analyzed by measuring cytochrome *c* release from mitochondria into the cytoplasm. Mitochondrial and cytoplasmic fractions were prepared using the Mitochondrial Fractionation Kit (Active Motif, Carlsbad, CA). Purity of extracts was analyzed by immunoblotting using cytoplasmic (GAPDH) and mitochondrial (V-β) markers. Cytochrome *c* levels in cytoplasm were also measured colorimetrically using a commercially available kit (FunctionELISA™ Cytochrome *c* kit, Active Motif; [25]).

2.9. Bcl-2, Bcl-x, Bax and Survivin expression

Levels of Survivin (whole cell homogenates), Bcl-2 and Bcl-xL (whole cell homogenates and mitochondrial fraction), and Bax (cytoplasmic and mitochondrial fractions) were analyzed by immunoblotting. α-Tubulin, GAPDH and V-β served as loading and purity controls.

2.10. WISP1 mRNA expression

WISP1 mRNA expression was analyzed by northern blotting as previously described [18; 19]. In brief, 20 μg of total RNA per lane were denatured, transferred onto nitrocellulose membrane, UV fixed, and probed with ^{32}P-labeled WISP1 cDNA. 28S rRNA served as an loading control.

2.11. Cell death detection

Cardiomyocytes in media containing 0.5% bovine serum albumin were treated with DOX for 24 h. Cell death was analyzed by a photometric enzyme immunoassay (Cell Death Detection ELISA^{PLUS} kit, Roche Applied Science;[25]). The assay is based on the quantitative sandwich enzyme immunoassay principle using mouse monoclonal antibodies directed against DNA and histones. Cell viability was confirmed by a microplate-based MTT cell viability assay[25], and viability was expressed as percentage of MTT absorbance at 562/650 nm in the absence of DOX. To investigate whether WISP1 blunts DOX-mediated cardiomyocyte death, cells were incubated with various concentrations of rhWISP1 for 1 h prior to DOX addition.

2.12. Data Analysis

Results are expressed as means ± S.E. For statistical analysis we used analysis of variance followed by an appropriate post hoc multiple comparison test (Tukey method). Data were considered statistically significant at $p < 0.05$.

3. Results

3.1. WISP1 blocks DOX-induced cardiomyocyte death

At a concentration of 1 μM, DOX induced internucleosomal degradation and cell death in adult mouse cardiomyocytes (Fig. 1A). The pro-apoptotic effect of DOX on cardiomyocytes was confirmed using the MTT assay that quantifies cell viability (Fig. 1B). Preincubation with WISP1 significantly attenuated DOX-mediated cardiomyocyte death in a concentration-dependent manner (Fig. 1A), with a significant cell survival effect detectable at 1 ng/ml, and a more pronounced effect at 10 ng/ml. A further increase to 100 ng/ml failed to demonstrate additional survival effects. Therefore, in all subsequent studies, WISP1 was used at 10 ng/ml. These results indicate that WISP1 is a potent pro-survival factor that can inhibit DOX-induced cardiomyocyte death (Fig. 1).

3.2. DOX induces cardiomyocyte death via p53 activation

p53, a stress-responsive, tumor suppressor protein, plays a critical role in regulating both cell survival and death [11;12]. DOX, at 1 μg/ml, significantly increased p53 protein levels, with peak levels detected at 3 h (Fig. 2A; densitometric analysis of three independent experiments are summarized in the lower panel). Further, DOX increased p53 DNA binding activity (Fig. 2*B*), its translocation to the nucleus (Fig. 2*C*), and stimulated p53-dependent reporter gene activity (Fig. 2*D*). Importantly, forced expression of mutant p53 (Ad.mp53) or incubation with the p53 inhibitor PFT-α significantly reversed DOX-mediated cardiomyocyte death (Fig. 2*E*), indicating that DOX is a potent inducer of p53 activation, and stimulates cardiomyocyte death in a p53-dependent manner (Fig. 2).

3.3. DOX activates pro-apoptotic signaling

Having demonstrated that DOX is a potent inducer of cardiomyocyte death (Fig. 1), and that DOX-induced cell death is mediated via p53 activation (Fig. 2), we next investigated the effects of DOX on various pro-apoptotic factors mediating cell death. Bax, a cell death factor, resides in cytoplasm and upon activation translocates to the mitochondria, damages the outer mitochondrial membrane, and is thus an intermediate in the intrinsic apoptotic signaling pathway [26]. Treatment with DOX promoted the translocation of Bax from cytoplasm to mitochondria in a time-dependent manner (Fig. 3A), with peak levels detected in the mitochondria around 8 h. Concomitantly, cytoplasmic levels were significantly depleted. Damage to the outer mitochondrial membrane promotes release of proteins that are normally constrained within the intermembranous space into the cytoplasm (*e.g.*, cytochrome *c*). Upon release into cytoplasm, cytochrome *c* triggers the activation of initiator caspases, leading to cell death [27]. In the cardiomyocytes, DOX stimulated cytochrome *c* release into cytoplasm (Fig. 3A, and confirmed by FunctionELISA™ in Fig. 3*B*), an effect that was significantly inhibited by the pancaspase inhibitor Z-VAD-fmk (Fig. 3*B*). Purity of cytoplasmic extracts was confirmed by a positive signal for GAPDH, and absence of V-β expression on immunoblotting (Fig.3*B*, inset). Since released cytochrome *c* stimulates caspase-3 activation [27], proteolytic cleavage of PARP, and DNA fragmentation, we next investigated the effects of DOX on these pro-apoptotic activities. DOX indeed stimulated caspase-3 activation (Fig. 3*C*), proteolytic cleavage of PARP (Fig. 3*D*; percent cleavage is shown in the right hand panel) and DNA fragmentation (Fig. 3*E*), effects that were significantly attenuated by the pancaspase (Z-VAD-fmk) and caspase-3 (Z-DEVD-fmk) inhibitors. These results indicate that DOX is a potent inducer of cell death, and induces cardiomyocyte death via translocation of Bax, and activation of both caspase-3 and PARP (Fig. 3).

3.4. DOX blunts anti-apoptotic signaling mechanisms

In the resting cell, pro-apoptotic mechanisms are kept in check by anti-apoptotic factors such as Bcl-2 and Bcl-xL [26]. Therefore, we investigated the effect of DOX on these pro-survival factors. Under basal conditions, cardiomyocytes contained relatively high levels of Bcl-2, and treatment with DOX significantly inhibited Bcl-2 expression (Fig. 4A; results from three independent experiments are summarized in the lower panel). Similarly, DOX significantly inhibited the expression of the anti-apoptotic Bcl-xL (Fig. 4B; results from three independent experiments are summarized in the lower panel). In contrast, DOX stimulated Bcl-xS, an alternatively spliced version of Bcl-x that exerts potent pro-apoptotic effects (Fig. 4B). Akt/PKB plays a central role in various cell growth response mechanisms [28]. Results in Fig. 4C demonstrate that DOX suppressed pAkt (Thr308) levels, without significantly altering total Akt levels at this time period (results from three independent experiments are summarized in the lower panel). GSK3β, a substrate of Akt, is retained in the cytoplasm in its non-phosphorylated active form, complexed with β-catenin, APC and axin [29;30;31]. Upon phosphorylation by Akt, pGSK3β dissociates from β-catenin, promoting β-catenin nuclear

translocation and induction of genes involved in cell survival and growth [29;30]. Results in Fig. 4D show that DOX suppressed pGSK3β (Ser9) levels in cardiomyocytes (results from three independent experiments are summarized in the lower panel), suggesting that treatment with DOX maintains GSK3β in an unphosphorylated active form. Since DOX inhibited Bcl-2 levels (Fig. 4A), we next verified whether DOX increases Bcl-2 degradation by the proteasome, as was reported previously in human umbilical vein endothelial cells [32]. Therefore, cardiomyocytes were incubated with the proteasomal inhibitor lactacystin prior to DOX addition. Our results show that preincubation with lacatcystin blocked DOX-mediated Bcl-2 degradation (Fig. 4E; results from three independent experiments are summarized in the lower panel). In contrast, lactacystin failed to significantly alter DOX induced Bcl-xL protein levels (Fig. 4F; results from three independent experiments are summarized in the lower panel), suggesting that proteasomal degradation plays a role in DOX-mediated inhibition of Bcl-2, but not Bcl-xL, expression in cardiomyocytes. Together, these results indicate that DOX negatively regulates expression and activation of various pro-survival factors in cardiomyocytes (Fig. 4).

3.5. WISP1 antagonizes DOX-mediated cardiomyocyte death via activation of PI3K-Akt signaling

We and others have previously demonstrated that WISP1 is a potent activator of PI3K and Akt, two critical players in cell survival and growth [17;18;19;20]. Therefore, we investigated whether WISP1 inhibits DOX-mediated cardiomyocyte death via activation of these intermediaries. Treatment with WISP1 significantly increased PI3K activity in cardiomyocytes (Fig. 5A), and induced Akt activation in a time-dependent fashion. WISP1 induced Akt phosphorylation (Fig. 5B) and enhanced its kinase activity (Fig. 5C). Forced expression of dnAkt (Fig. 5D), dnPI3Kp85 (Fig. 5E) or treatment with the Akt inhibitor Akti-X (Fig. 5D), or the PI3K inhibitors Ly294002 and wortmannin (Fig. 5F) attenuated WISP1-induced Akt phosphorylation. Importantly, inhibition of Akt and PI3K by the forced expression of dnAkt and dnPI3Kp85 reversed WISP1 pro-survival effects in DOX-treated cardiomyocytes (Fig. 5G). Our results also demonstrated that forced expression of constitutively active Akt (myr.Akt) recapitulates the prosurvival effects of WISP1, and inhibits DOX-induced cell death (Fig. 5H). Together, these results indicate that WISP1 reverses DOX-mediated cardiomyocyte death via PI3K-dependent Akt activation (Fig. 5).

3.6. WISP1 reverses DOX activated pro-apoptotic signaling

We have demonstrated that DOX activates various pro-apoptotic signaling molecules (Fig. 3). Since WISP1 attenuates DOX-mediated cell death (Fig. 1), we investigated whether WISP1 exerts its pro-survival effects by reversing the DOX-mediated activations of p53 and Bax. Pre-treatment with 10 ng/ml WISP1 significantly attenuated DOX-mediated p53 activation (Fig. 6A) and p53-dependent reporter gene activation (Fig. 6B). Similarly, WISP1 inhibited DOX-mediated translocation of Bax to the mitochondria (Fig. 6C; results from three independent experiments are summarized in the right hand panel). Further, WISP1 blocked DOX-induced cytochrome *c* release (Fig. 6D), activation of caspase-3 (Fig. 6E) and PARP cleavage (Fig. 6F; percent cleavage is shown in the right hand panel). These results indicate that WISP1 is a potent pro-survival factor that inhibits DOX-induced cardiomyocyte death by reversing activations of pro-apoptotic p53 and Bax, and inhibiting cytochrome *c* release (Fig. 6).

3.7. WISP1 reverses DOX-induced mitogen-activated protein kinase (MAPK) activation

Both p38 MAPK and JNK play critical roles in cell death pathways. They phosphorylate Bax and promote its translocation to mitochondria [33]. We investigated whether p38MAPK and JNK mediate DOX-induced cardiomyocyte death, and whether WISP1 can reverse this phenomenon. Our results show that indeed DOX stimulates p38 MAPK phosphorylation (Thr180/Tyr182) in a time-dependent manner (Fig. 7A), and this effect is significantly inhibited

by SB 203580 (SB; Fig. 7B). Further, DOX activated JNK (pJNK Thr183/Tyr185, Fig. 7C) and this was inhibited by SP 600125 (SP; Fig. 7D). Treatment with SB and SP attenuated DOX-induced Bax translocation to mitochondria (Fig. 7E) and inhibited cell death (Fig. 7F). Importantly, WISP1 reversed DOX-induced p38 MAPK (p-p38 MAPK Thr180/Tyr182, Fig. 7G) and JNK (pJNK Thr183/Tyr185, Fig. 7H) activations, indicating that WISP1 inhibits DOX-induced cardiomyocyte death by inhibiting activation of MAPK and mitochondria-associated intrinsic apoptotic mechanisms (Fig. 7).

3.8. WISP1 restores the anti-apoptotic signaling mechanism attenuated by DOX

We have shown that while DOX inhibits anti-apoptotic Bcl-2 and Bcl-xL expression in cardiomyocytes, it also induces the expression of the pro-apoptotic Bcl-xS (Fig. 4). Since WISP1 inhibits pro-apoptotic signaling [18;19;20], we next investigated whether it also restores anti-apoptotic signaling. Treatment with WISP1 inhibited DOX-mediated suppression of Bcl-2 expression (Fig. 8A; results from three independent experiments are shown in the lower panel), thus reducing the Bax to Bcl-2 ratios in whole cell homogenates (Fig. 8B). Similarly, by restoring mitochondrial Bcl-2 levels (Fig. 8C), WISP1 also reduced Bax to Bcl-2 ratios in mitochondrial fraction (Fig. 8C, lower panel). In an analogous manner, it also restored Bcl-xL expression (Fig. 8D; results from three independent experiments are shown in the lower panel) and reduced Bax to Bcl-xL ratio (Fig. 8E). Similarly, by restoring mitochondrial Bcl-xL levels (Fig. 8F), WISP1 reduced Bax to Bcl-xL ratios (Fig. 8F, lower panel). Importantly, forced expression of wild-type Bcl-2 or Bcl-xL mimicked WISP1 treatment, and inhibited DOX-induced cardiomyocyte death (Fig 8G; expression levels of Bcl-2 ad Bcl-xL following adenoviral transduction are shown in panel 8H). These results indicate that WISP1 can exert prosurvival effects by restoring DOX-mediated suppression of Bcl-2 and Bcl-xL expression (Fig. 8).

3.9. WISP1 induces Survivin expression in PI3K-Akt dependent manner

Survivin is a member of the ‘inhibitor of apoptosis’ (IAP) gene family[34]. It promotes cell survival via activation of diverse signal transduction pathways. It also physically associates with and inhibits executioner caspases such as caspase-3[35]. Since WISP1 activates PI3K and Akt (Fig. 5), and as Akt regulates the expression of various pro-survival factors, including Survivin, we investigated whether WISP1 induces Survivin expression, and investigated the underlying mechanisms. DOX suppressed Survivin protein expression (*versus* basal levels), an effect that was significantly inhibited by WISP1 pretreatment (Fig. 9A). In fact, at 10 and 100 ng/ml, WISP1-induced Survivin expression was 3-4 fold higher than that seen at basal levels. Further, forced expression of dnAkt and dnPI3Kp85 significantly inhibited WISP1-induced Survivin protein expression (Fig. 9B). Since Survivin is a potent anti-apoptotic factor, we next investigated whether forced expression of wild-type Survivin mimics WISP1 pretreatment, and whether its overexpression antagonizes DOX-mediated cardiomyocyte death. Cardiomyocytes were transduced with either wild-type or mutant Survivin for 24 h (expression levels of wild-type and mutant Survivin following adenoviral transduction are shown in Fig. 9C), and then treated with DOX. Survivin significantly attenuated DOX-mediated cardiomyocyte death (Fig. 9D), possibly via inhibition of DOX-mediated caspase-3 activation (Fig. 9E). These results demonstrate that WISP1 induces Survivin expression via PI3K-Akt-dependent signaling, and WISP1 antagonizes cardiomyocyte death in part via Survivin (Fig. 9).

3.10. WISP1 induces GSK3β phosphorylation and β-catenin nuclear translocation

Since phosphorylation and degradation of GSK3β leads to β-catenin nuclear translocation and induction of genes involved in cell survival, and since DOX inhibits pGSK3β (Ser9) levels, we next determined whether WISP1 reverses this response. Results in Fig. 10A show that

WISP1 indeed induced GSK3β phosphorylation (Ser9) in a time-dependent manner, an effect that was attenuated by the GSK3β-specific inhibitor SB-216763, and by LiCl (Fig. 10B). Further, WISP1 induced GSK-3β phosphorylation (Ser9) via PI3K and Akt (Fig. 10C and 10D), and stimulated β-catenin nuclear translocation in a time-dependent manner (Fig. 10E). These results indicate that WISP1 induces PI3K-Akt-dependent GSK3β phosphorylation and β-catenin nuclear translocation in cardiomyocytes (Fig. 10).

3.11. WISP1 induces its own expression

Since WISP1 is a β-catenin-responsive gene [30], we next investigated whether WISP1 can induce its own expression. Under basal conditions, cardiomyocytes express WISP1 at low levels, and treatment with WISP1 increased its own mRNA expression (Fig. 10F). A significant increase in WISP1 mRNA expression was detected by 3h, and peaked at 12 h. These effects were significantly attenuated by WISP1 neutralizing antibodies, but not by the control IgG (Fig. 10F). Similarly, treatment with WISP1 elevated WISP-1 protein expression in a time–dependent manner, with peak levels detected at 12 h (Fig. 10G). These results demonstrate that WISP1 induces its own expression in cardiomyocytes (Fig. 10).

4. Discussion

Doxorubicin is a potent chemotherapeutic agent used in the treatment of various childhood and adult malignancies. It can however induce both acute and chronic cardiotoxicity as manifested by cardiomyocyte death, progressive cardiomyopathy, and congestive heart failure [1;2;3;4]. Here we show that DOX induced cell death in adult mouse cardiomyocytes is attenuated by pretreatment with WISP1. WISP inhibited DOX-mediated p53 activation, p38 MAPK and JNK phosphorylation, mitochondrial translocation of Bax, activation of caspase-3, and suppression of Bcl-2 and Bcl-xL. It also induced PI3K-dependent Akt activation, PI3K-Akt-dependent Survivin expression, GSK3β phosphorylation, and β-catenin nuclear translocation. Importantly, WISP1 induced its own expression (Fig. 11). These results provide important insights into the cytoprotective effects of WISP1 in cardiomyocytes, and suggest a potential therapeutic role for WISP1 in the prevention of DOX-induced cardiotoxicity.

Consistent with earlier studies [8;13;14], we found that DOX upregulated p53, and induced cardiomyocyte death in a p53-dependent manner. Treatment with PFT-α, the pharmacological inhibitor of p53, or forced expression of a mutant p53, abrogated DOX-induced cardiomyocyte death. The pathways whereby DOX induces cardiomyocyte cell death have not been fully explored, however it has been shown that DOX can induce p53 activation in cardiomyocytes by markedly inhibiting its ubiquitin-dependent proteasomal degradation [36], as well as by stabilizing p53 by enhancing proteasomal degradation of the coactivator p300 [36]. DOX induces p300 phosphorylation and degradation in a p38 MAPK-dependent manner. We found that pretreatment of the cells with WISP1 induced PI3K and Akt activation. It has been reported that activation of PI3K enhances p300 metabolic stability [37], and inhibition of PI3K promotes p300 degradation via the 26S proteasome pathway [37]. Further, activation of Akt has also been shown to maintain the steady-state levels of p300 [37], Thus one mechanism whereby WISP1 counteracts the effects of DOX in cardiomyocytes may be by stabilizing p300 via PI3K-Akt signaling.

In addition to nuclear localization, p53 has also been shown to translocate to mitochondria and stimulate the intrinsic (mitochondrial) cell death pathway [6;7;10]. We found that DOX stimulated mitochondrial translocation of Bax, a p53-regulated pro-apoptotic gene product, and this was significantly inhibited by WISP1. Bax exists in cytoplasm as a 21-kDa monomer [38;39] and following activation, it translocates to the mitochondrial outer membrane, induces mitochondrial permeability transition pores, and stimulates release of cytochrome *c*, Smac/DIABLO, and other apoptosis-inducing factors [38;39]. Cytochrome *c* has a critical role in cell

survival, since following release into cytoplasm, it initiates the formation of apoptosomes and the subsequent activation of caspases 9 and 3, and caspase-dependent extrinsic cell death pathways [27]. We found that WISP1 inhibited DOX-induced cytochrome *c* release, caspase 3 activation and PARP cleavage, indicating that WISP1 inhibits both intrinsic as well as extrinsic cell death pathways.

Activation of Bax is regulated by site-specific serine/ threonine phosphorylation. Both p38 MAPK and JNK have been shown to induce Bax activation and mitochondrial translocation via phosphorylation of threonine 167 (Thr167) [33]. In our study, DOX activated p38 MAPK and JNK, and these kinases mediated Bax translocation to mitochondria. Importantly, WISP1 treatment blocked Bax translocation. The mechanisms are unclear, but could involve inhibition of MAPKs, or perhaps PI3K-Akt-dependent Bax phosphorylation at Ser184, which would prevent Bax from heterodimerizing with Bcl-xL and other anti-apoptotic factors [40]. By inhibiting GSK3β activation, WISP1 could also block Bax phosphorylation at Ser163 and consequently its activation [41].

Bcl-2 and Bcl-xL are potent pro-survival factors. Bcl-xS, on the other hand, an alternatively spliced variant of the Bcl-x gene, exerts pro-apoptotic effects. Here we show that DOX inhibits Bcl2 and Bcl-xL, but induces Bcl-xS expression. Though we have not investigated the underlying signaling mechanisms, a number may have possibly contributed to this differential regulation. For example, DOX has been shown to activate the sphingomyelinceramide pathway in cardiomyocytes [42]. Ceramide is a sphingosine-based lipid signaling molecule that can activate protein phosphatase 1 (PP1). PP1 is known to act on serine/arginine (SR)-rich proteins which are involved in regulating and selecting splice sites in Bcl-x pre mRNA [43], thus favoring Bcl-xS production. Interestingly, DOX has been shown to significantly increase PP1 in hearts [44]. DOX also inhibits PKCα at both protein and activity levels [45]. Ceramide-activated PP1 inhibits PKCα, and inactivates SB1, a respressor located 187 nucleotides upstream of the Bcl-xS 5' splice site [46], thus favoring Bcl-xS transcription. Activation of p53 has also been shown to negatively regulate Bcl-2 transcription by targeting the TATA sequence in its P2 minimal promoter. It is also possible that DOX might downregulate Bcl2 transcription by depleting GATA4, a cardiac-enriched transcription factor essential for various physiological and adaptive responses. The Bcl2 promoter contains two GATA binding sites at -266 and -1025 [47], and GATA4 is also reported to be an upstream activator of Bcl-xL. Since GATA4 activation is mediated by PI3K/Akt [48;49], and since DOX suppresses pAkt (Thr308) levels, it is plausible that DOX might down regulate Bcl-2 and Bcl-xL expressions via reduced Akt activation.

GSK3β regulates a variety of signaling pathways and cellular processes including cardiomyocyte growth and survival. In the resting cell, GSK3β is catalytically active and is complexed with β-catenin, APC and axin. In this configuration, it phosphorylates β-catenin and promotes its ubiquitination and degradation [29]. However, following Akt-mediated GSK3β phosphorylation and degradation, liberated β-catenin translocates to the nucleus where it forms complexes with various transcription factors, particularly T-cell-specific transcription factor/lymphoid enhancer binding factor 1 (TCF/LEF1), and induces TCF/LEF1-dependent gene expression. Here we show that WISP1 induces GSK3β phosphorylation, β-catenin nuclear translocation, and the transcription of its own gene. Although the *WISP1 cis* regulatory region contains multiple TCF/LEF1 binding sites [30], and it would seem possible that the WISP1-GSK3β-β-catenin signaling might contribute to *WISP*1 autoregulation, previous studies suggest that these TCF/LEF1 sites play only a minor role in *WISP1* transcription [30]. Interestingly, we and others have shown that *WISP1* is a CREB-responsive gene [18;30], and that the CREB site is critical for β-catenin-induced *WISP1* transcription [30]. However, it is not known whether WISP1 activates CREB directly or induces its activation via intermediaries,

therefore the precise mechanism responsible for WISP1 autoregulation remains to be determined.

WISP1 also induced Survivin expression in the cardiomyocytes. Survivin is a member of the Inhibitor of Apoptosis family, and exerts its pro-survival effects by directly interacting with Smac/DIABLO, an important pro-apoptotic factor [34]. Further, we showed that overexpression of wild-type Survivin blunted the effect of DOX, whereas overexpression of mutant Survivin had a potentiating effect. Previous studies have shown that DOX inhibits Survivin expression via activation of p53 [50]. Since we have demonstrated that WISP1 inhibits p53 and induces Survivin expression via PI3K and Akt, this may be one of the more important mechanisms mediating the WISP1 protective effect. It has also been reported that p53 negatively regulates PI3K transcription, translation and activation [51]. It is thus possible that WISP1-mediated p53 downregulation might have contributed to PI3K and Akt activations, and PI3K-Akt-dependent Survivin expression. Of note, Survivin has also been reported to negatively regulate p53 expression [52]. This suggests a sustained inhibition of p53 by WISP1-Survivin signaling in DOX-treated cardiomyocytes. It has also been reported that activated GSK3β promotes nuclear localization of Survivin [53]. However, upon nuclear localization, Survivin loses its anti-apoptotic potential, and induces cell cycle arrest and apoptosis in some cancer cells [53]. Since WISP1 induces GSK3β phosphorylation, and thus targeting its degradation by the ubiquitin-proteasome system, we hypothesize that treatment with WISP1 favors cytoplasmic localization of Survivin.

Our preliminary studies demonstrate that treatment of cardiomyocytes with WISP1 suppresses the dual specificity phosphatase PTEN, a negative regulator of PI3K, in cardiomyocytes. Whether, this suppression is p53 dependent is not known. Studies are in progress to determine whether WISP1-mediated PTEN downregulation is p53-dependent, and whether PTEN suppression upregulates Survivin expression in PI3K-dependent manner [54]. Of note, endogenous PTEN has been shown to suppress Survivin expression [55]. Our preliminary studies also demonstrated that WISP1 induces neuregulin-1 expression and secretion in cardiomyocytes. Since neuregulin-1 exerts pro-survival and pro-mitogenic effects in cardiomyocytes [56], we are actively pursuing the underlying molecular mechanisms involved in WISP1-mediated neuregulin-1 induction and whether WISP1-neuregulin-1 signaling antagonizes DOX-induced cardiomyocyte death.

In summary, our results provide important insights into the cytoprotective effects of WISP1 in cardiomyocytes, and suggest a potential therapeutic role for WISP1 in DOX-induced cardiotoxicity.

Supplementary Material

Refer to Web version on PubMed Central for supplementary material.

Acknowledgments

This work was supported in part by National Heart, Lung, and Blood Institute Grant HL-86787 (Chandrasekar), HL070241 and HL080682 (Delafontaine), and by Award Number 1I01BX007080 from the Biomedical Laboratory Research & Development Service of the VA Office of Research and Development (Chandrasekar).

Abbreviations used

Bcl-2	B cell leukaemia-2
Bax	Bcl-2 -associated x protein
Bcl-xL	B cell leukemia-x long

CCN	Cyr61/CTGF/Nov
Cyr61	cysteine-rich protein 61
CTGF	connective tissue growth factor
Nov	nephroblastoma-overexpressed gene
CREB	CRE-bindingprotein
DIABLO	direct IAP binding protein with low pI
DOX	doxorubicin
IAP	inhibitor of apoptosis
JNK	Jun N-terminal kinase
PDK1	phosphoinositide-dependent kinase-1
GSK	glycogen synthase kinase
MOI	multiplicity of infection
MAPK	mitogen-activated protein kinase
MTT	(3-(4,5-dimethylthiazol-2-yl)-2,5-diphenyl-2H-tetrazolium bromide
PI3K	phosphoinositide 3-kinase
IAPs	inhibitor of apoptosis proteins
PKB	protein kinase B
Smack	Second mitochondria-derived activator of capsizes
PTEN	Phosphates and Tensing homologue deleted from chromosome Ten
GSK3β	glycogen syntheses kinas 3β
WISP	Wnt-1 inducible signaling pathway protein
WNT	wingless-type MMTV integration site family
SGK	serum and glucocorticoid-induced protein kinase
TCF/LEF	T-cell factor-lymphoid enhancer binding factor
WISP1	WNT1-inducible signaling pathway protein-1

References Cited

1. al-Shabanah O, Mansour M, el-Kashef H, al-Bekairi A. Biochem. Mol. Biol. Int 1998;45:419. [PubMed: 9678264]
2. Singal PK, Iliskovic N. N. Engl. J. Med 1998;339:900. [PubMed: 9744975]
3. Ferreira AL, Matsubara LS, Matsubara BB. Cardiovasc. Hematol. Agents Med. Chem 2008;6:278. [PubMed: 18855640]
4. Carvalho C, Santos RX, Cardoso S, Correia S, Oliveira PJ, Santos MS, Moreira PI. Curr. Med. Chem 2009;16:3267. [PubMed: 19548866]
5. Olson RD, Mushlin PS. FASEB J 1990;4:3076. [PubMed: 2210154]
6. Kotamraju S, Konorev EA, Joseph J, Kalyanaraman B. J. Biol. Chem 2000;275:33585. [PubMed: 10899161]
7. Salvatorelli E, Guarnieri S, Menna P, Liberi G, Calafiore AM, Mariggio MA, Mordente A, Gianni L, Minotti G. J. Biol. Chem 2006;281:10990. [PubMed: 16423826]

8. Chua CC, Liu X, Gao J, Hamdy RC, Chua BH. Am. J. Physiol. Heart Circ. Physiol 2006;290:H2606. [PubMed: 16687611]
9. L'Ecuyer T, Sanjeev S, Thomas R, Novak R, Das L, Campbell W, Heide RV. Am. J. Physiol. Heart Circ. Physiol 2006;291:H1273. [PubMed: 16565313]
10. Nithipongvanitch R, Ittarat W, Cole MP, Tangpong J, Clair DK, Oberley TD. Antioxid. Redox. Signal 2007;9:1001. [PubMed: 17508921]
11. Nithipongvanitch R, Ittarat W, Velez JM, Zhao R, St Clair DK, Oberley TD. J. Histochem. Cytochem 2007;55:629. [PubMed: 17312011]
12. Kruse JP, Gu W. Cell 2009;137:609–22. [PubMed: 19450511]
13. Lin Y, Waldman BC, Waldman AS. DNA Repair (Amst.) 2003;2:1. [PubMed: 12509264]
14. Shizukuda Y, Matoba S, Mian OY, Nguyen T, Hwang PM. Mol. Cell. Biochem 2005;273:25. [PubMed: 16013437]
15. Chen CC, Lau LF. Int. J. Biochem. Cell. Biol 2009;41:771. [PubMed: 18775791]
16. Yeger H, Perbal B. J. Cell. Commun. Signal 2007;1:159. [PubMed: 18568428]
17. Pennica D, Swanson TA, Welsh JW, Roy MA, Lawrence DA, Lee J, Brush J, Taneyhill LA, Deuel B, Lew M, Watanabe C, Cohen RL, Melhem MF, Finley GG, Quirke P, Goddard AD, Hillan KJ, Gurney AL, Botstein D, Levine AJ. Proc. Natl. Acad. Sci. USA 1998;95:14717. [PubMed: 9843955]
18. Venkatachalam K, Venkatesan B, Valente AJ, Melby PC, Nandish S, Reusch JE, Clark RA, Chandrasekar B. J. Biol. Chem 2009;284:14414. [PubMed: 19339243]
19. Colston JT, de la Rosa SD, Koehler M, Gonzales K, Mestril R, Freeman GL, Bailey SR, Chandrasekar B. Am. J. Physiol. Heart Circ. Physiol 2007;293:H1839. [PubMed: 17616748]
20. Su F, Overholtzer M, Besser D, Levine AJ. Genes Dev 2002;16:46. [PubMed: 11782444]
21. Thimmaiah KN, Easton JB, Germain GS, Morton CL, Kamath S, Buolamwini JK, Houghton PJ. J. Biol. Chem 2005;280:31924. [PubMed: 16009706]
22. Beaulieu JM, Sotnikova TD, Yao WD, Kockeritz L, Woodgett JR, Gainetdinov RR, Caron MG. Proc. Natl. Acad. Sci. USA 2004;101:5099. [PubMed: 15044694]
23. Venkatesan B, Valente AJ, Reddy VS, Siwik DA, Chandrasekar B. Am. J. Physiol. Heart Circ. Physiol 2009;297:H874. [PubMed: 19561311]
24. Mesri M, Wall NR, Li J, Kim RW, Altieri DC. J. Clin. Invest 2001;108:981. [PubMed: 11581299]
25. Chandrasekar B, Vemula K, Surabhi RM, Li-Weber M, Owen-Schaub LB, Jensen LE, Mummidi S. J. Biol. Chem 2004;279:20221. [PubMed: 14960579]
26. Gross A, Jockel J, Wei MC, Korsmeyer SJ. EMBO J 1998;17:3878. [PubMed: 9670005]
27. Li P, Nijhawan D, Budihardjo I, Srinivasula SM, Ahmad M, Alnemri ES, Wang X. Cell 1997;91:479. [PubMed: 9390557]
28. Miyamoto S, Murphy AN, Brown JH. J. Bioenerg. Biomembr 2009;41:169. [PubMed: 19377835]
29. Grimes CA, Jope RS. Prog. Neurobiol 2001;65:391. [PubMed: 11527574]
30. Xu L, Corcoran RB, Welsh JW, Pennica D, Levine AJ. Genes Dev 2000;14:585–95. [PubMed: 10716946]
31. Cross DA, Alessi DR, Cohen P, Andjelkovich M, Hemmings BA. Nature 1995;378:785. [PubMed: 8524413]
32. Dimmeler S, Breitschopf K, Haendeler J, Zeiher AM. J. Exp. Med 1999;189:1815. [PubMed: 10359585]
33. Kim BJ, Ryu SW, Song BJ. J. Biol. Chem 2006;281:21256–65. [PubMed: 16709574]
34. Verdecia MA, Huang H, Dutil E, Kaiser DA, Hunter T, Noel JP. Nat. Struct. Biol 2000;7:602. [PubMed: 10876248]
35. Tamm I, Wang Y, Sausville E, Scudiero DA, Vigna N, Oltersdorf T, Reed JC. Cancer Res 1998;58:5315. [PubMed: 9850056]
36. Morimoto T, Fujita M, Kawamura T, Sunagawa Y, Takaya T, Wada H, Shimatsu A, Kita T, Hasegawa K. Circ. J 2008;72:1506. [PubMed: 18724031]
37. Chen J, Halappanavar SS, St-Germain JR, Tsang BK, Li Q. Cell. Mol. Life Sci 2004;61:1675. [PubMed: 15224190]
38. Desagher S, Martinou JC. Trends Cell. Biol 2000;10:369. [PubMed: 10932094]

39. Wei MC, Zong WX, Cheng EH, Lindsten T, Panoutsakopoulou V, Ross AJ, Roth KA, MacGregor GR, Thompson CB, Korsmeyer SJ. Science 2001;292:727. [PubMed: 11326099]
40. Gardai SJ, Hildeman DA, Frankel SK, Whitlock BB, Frasch SC, Borregaard N, Marrack P, Bratton DL, Henson PM. J. Biol. Chem 2004;279:21085. [PubMed: 14766748]
41. Linseman DA, Butts BD, Precht TA, Phelps RA, Le SS, Laessig TA, Bouchard RJ, Florez-McClure ML, Heidenreich KA. J. Neurosci 2004;24:9993. [PubMed: 15525785]
42. Delpy E, Hatem SN, Andrieu N, de Vaumas C, Henaff M, Rucker-Martin C, Jaffrezou JP, Laurent G, Levade T, Mercadier JJ. Cardiovasc. Res 1999;43:398. [PubMed: 10536670]
43. Chalfant CE, Rathman K, Pinkerman RL, Wood RE, Obeid LM, Ogretmen B, Hannun YA. J. Biol. Chem 2002;277:12587. [PubMed: 11801602]
44. Fan GC, Zhou X, Wang X, Song G, Qian J, Nicolaou P, Chen G, Ren X, Kranias EG. Circ. Res 2008;103:1270. [PubMed: 18948619]
45. Jin JS, Yao CW, Chin TY, Chueh SH, Lee WH, Chen A. Am. J. Physiol. Renal Physiol 2004;287:F188. [PubMed: 15113750]
46. Revil T, Toutant J, Shkreta L, Garneau D, Cloutier P, Chabot B. Mol. Cell. Biol 2007;27:8431. [PubMed: 17923691]
47. Kobayashi S, Lackey T, Huang Y, Bisping E, Pu WT, Boxer LM, Liang Q. FASEB J 2006;20:800. [PubMed: 16469847]
48. Zhao W, Kitidis C, Fleming MD, Lodish HF, Ghaffari S. Blood 2006;107:907. [PubMed: 16204311]
49. Condorelli G, Drusco A, Stassi G, Bellacosa A, Roncarati R, Iaccarino G, Russo MA, Gu Y, Dalton N, Chung C, Latronico MV, Napoli C, Sadoshima J, Croce CM, Ross J Jr. Proc. Natl. Acad. Sci. USA 2002;99:12333. [PubMed: 12237475]
50. Song Z, Liu S, He H, Hoti N, Wang Y, Feng S, Wu M. Mol. Biol. Cell 2004;15:1287. [PubMed: 14699067]
51. Singh B, Reddy PG, Goberdhan A, Walsh C, Dao S, Ngai I, Chou TC, P OC, Levine AJ, Rao PH, Stoffel A. Genes Dev 2002;16:984. [PubMed: 11959846]
52. Wang Z, Fukuda S, Pelus LM. Oncogene 2004;23:8146. [PubMed: 15361831]
53. Li J, Xing M, Zhu M, Wang X, Wang M, Zhou S, Li N, Wu R, Zhou M. Cancer Lett 2008;272:91. [PubMed: 18701211]
54. Guha M, Plescia J, Leav I, Li J, Languino LR, Altieri DC. Cancer Res 2009;69:4954. [PubMed: 19470765]
55. Li Y, Tennekoon GI, Birnbaum M, Marchionni MA, Rutkowski JL. Mol. Cell. Neurosci 2001;17:761. [PubMed: 11312610]
56. Bersell K, Arab S, Haring B, Kuhn B. Cell 2009;138:257. [PubMed: 19632177]

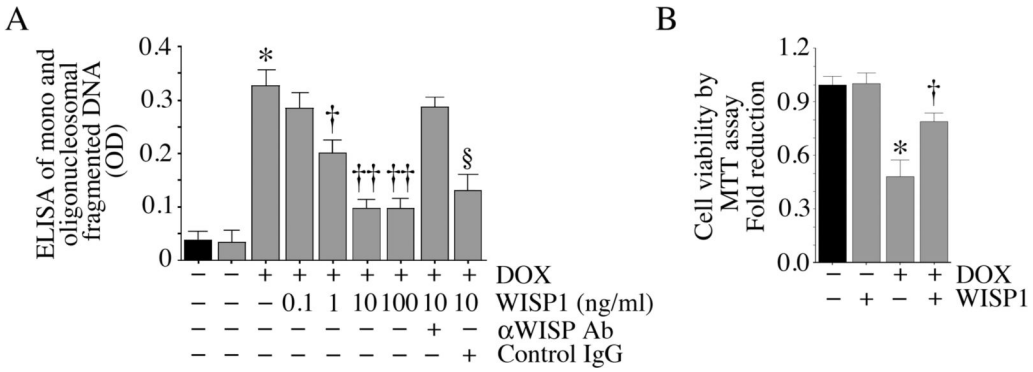

Fig. 1. WISP1 attenuates DOX-mediated cardiomyocyte death

A, DOX induces cardiomyocyte death. Adult mouse cardiomyocytes were treated with rhWISP1 at the indicated concentrations for 1 h prior to addition of DOX (1 μM for 24 h). Specificity of WISP1 activity was verified by incubating WISP1 with neutralizing antibodies or control IgG (10 μg/ml for 1 h) before addition. Mono and oligonucleosomal fragmented DNA in cytoplasmic extracts was quantified by an ELISA as described in 'Materials and methods'. **P* < 0.001 *versus* untreated, †*P* < 0.05, ††*P* < 0.001 *versus* DOX alone (n=12). *B*, DOX-mediated cell death by MTT cell viability assay. Cardiomyocytes were treated with WISP1 (10 ng/ml for 1 h) prior to DOX addition (1 μM for 24 h). Cell viability was assessed by the MTT assay. **P* < 0.001 *versus* untreated, †*P* < 0.01 *versus* DOX (n=12).

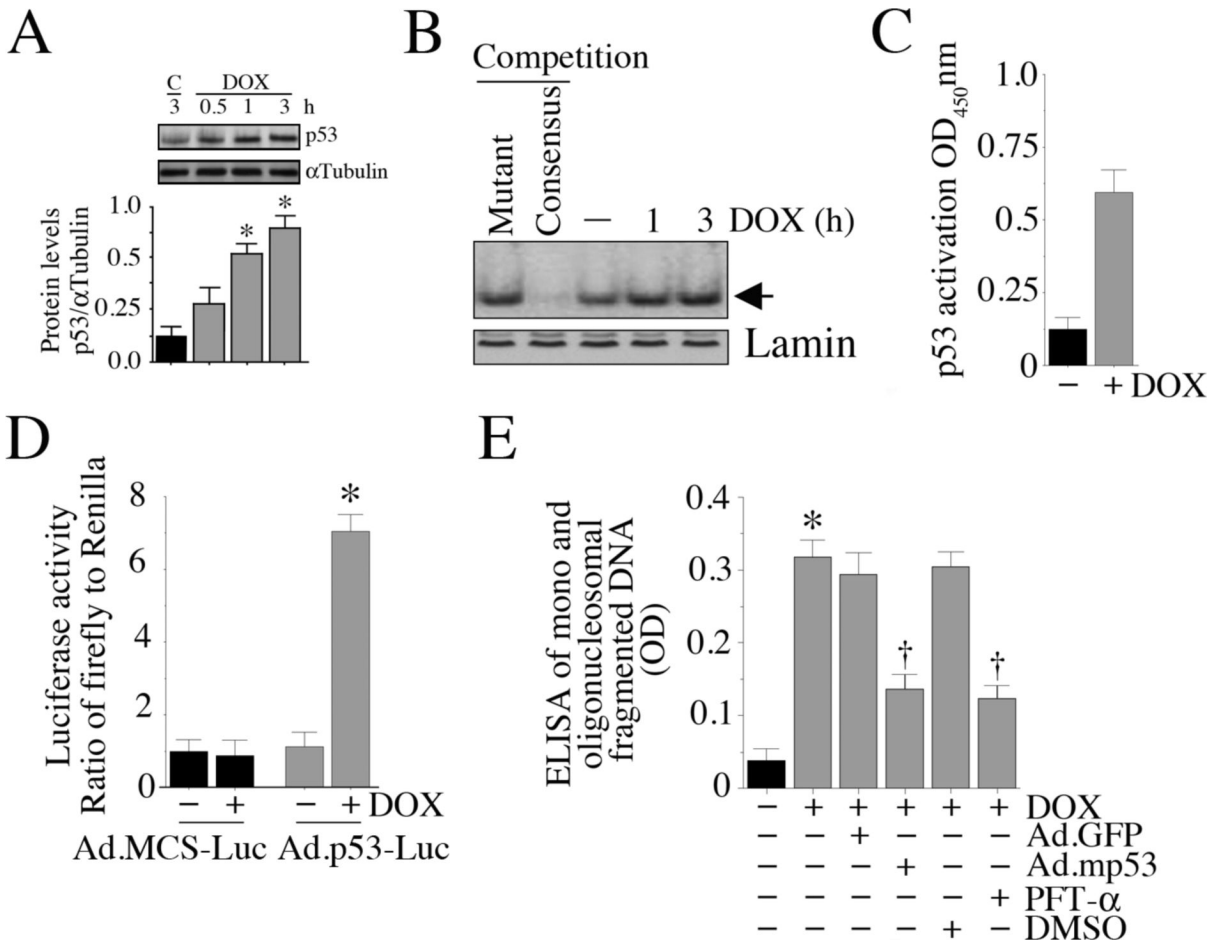

Fig. 2. DOX activates p53

A, DOX induces p53 expression in a time-dependent manner. Cardiomyocytes were treated with DOX for the indicated periods, and p53 levels analyzed by immunoblotting of whole cell homogenates. αTubulin served as a loading control. Results from three independent experiments are summarized in the lower panel. **P* < 0.001 *versus* control (C) at 3 h. *B*, DOX stimulates p53 DNA binding activity. Nuclear proteins extracted from cardiomyocytes treated as in *A* were analyzed for p53 DNA binding activity by EMSA using ^{32}P-labeled double stranded consensus p53 oligonucleotides (indicated by an arrow). Binding specificity of p53 DNA was shown by competition with 50-fold molar excess of unlabeled double-stranded mutant p53 oligonucleotide, Lane 1, and 50-fold molar excess of cold consensus p53 oligonucleotide, Lane 2. Lamin served as a loading control (n=3). *C*, DOX-induced p53 activation was quantified by ELISA. Nuclear extracts described in *B* (DOX for 3 h) were analyzed for p53 activation by ELISA, as described under 'Materials and methods'. **P* < 0.001 *versus* untreated (n=3/group). *D*, DOX stimulates p53-dependent reporter gene activity. Cardiomyocytes were transduced with Ad-p53-Luc (MOI 50), or Ad-MCS-Luc (MOI 50) as control; Ad.pRL-Luc (MOI 50) served as an internal control. After 24 h, the cells were treated with DOX (1 μM- for 7 h), and firefly and *Renilla* luciferase activities were determined. **P* < 0.001 *versus* Untreated (n=6/group). *E*, Forced expression of mutant p53 inhibits DOX-mediated cardiomyocyte death. Cardiomyocytes transduced with adenoviral mutant p53 (MOI 100 for 24 h) were treated with DOX for 24 h. Ad.GFP served as a control. Cell death was analyzed by ELISA. **P* < 0.001 *versus* untreated, †*P* < 0.01 *versus* DOX (n=12/group).

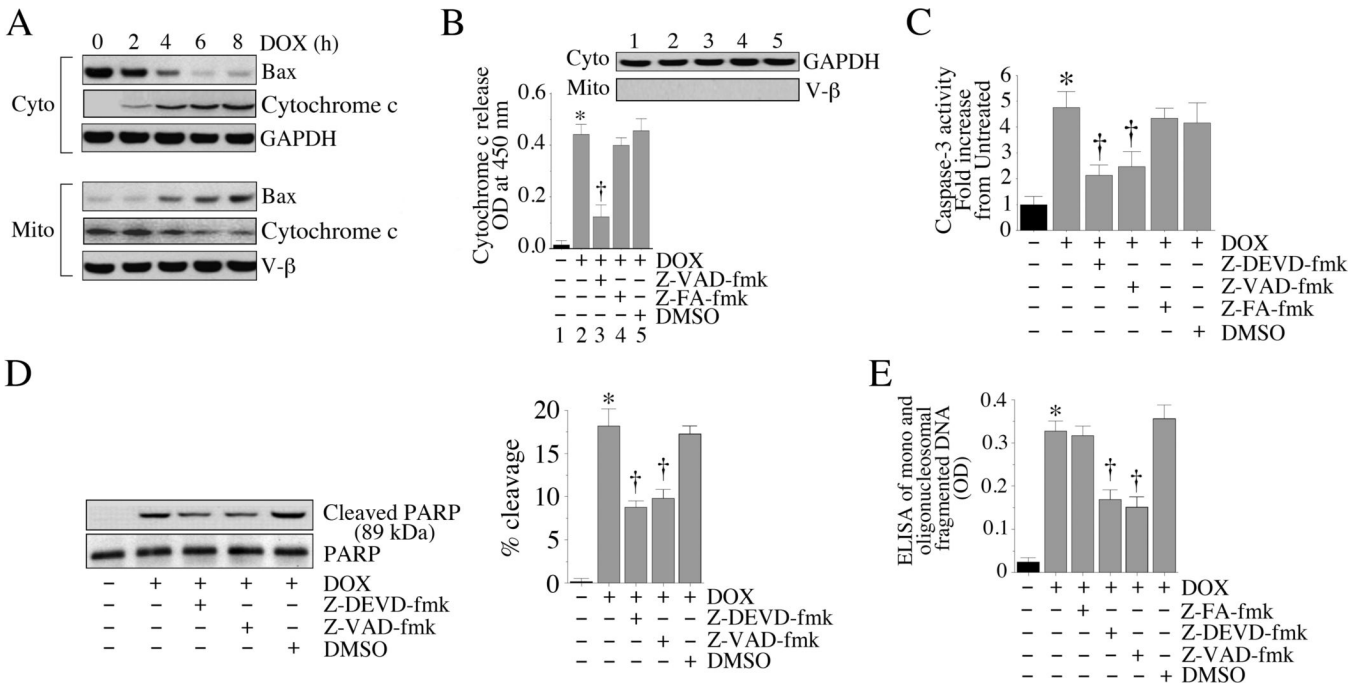

Fig. 3. DOX activates pro-apoptotic signaling

A, DOX promotes Bax translocation to mitochondria and stimulates cytochrome c release into cytoplasm. Cardiomyocytes were treated with 1 μM DOX for the indicated time periods. Mitochondrial and cytoplasmic extracts were analyzed for Bax and cytochrome c levels by immunoblotting. Purity of extracts was verified by GAPDH (cytoplasmic) and V-β (mitochondrial) expressions by immunoblotting (n=3). *B*, DOX-mediated cytochrome *c* release is inhibited by the pancaspase inhibitor. Cardiomyocytes were treated with Z-VED-fmk (50 μM in DMSO for 30 min) followed by DOX (1 μM) for 8 h. Z-FA-fmk served as a negative control. DMSO served as a solvent control. Cytochome *c* levels in cytoplasmic extracts were analyzed by a colorimetric assay. Purity of cytoplasmic extracts and equal loading were confirmed by immunoblotting for GAPDH (inset). *$P < 0.001$ *versus* untreated, † $P < 0.01$ *versus* DOX (n=6/group). *C*, DOX activates caspase-3. Cardiomyocytes were treated with either caspase-3 (Z-DEVD-fmk or pancaspase (Z-VED-fmk) inhibitor prior to DOX addition (1 μM for 8 h). Z-FA-fmk served as a negative control. DMSO served as a solvent control. Caspase-3 activity was determined using a fluorescent method. * $P < 0.001$ *versus* untreated, † $P < 0.01$ *versus* DOX (n=6/group). *D*, DOX activates PARP. Cardiomyocytes treated as in *C* were analyzed for cleaved PARP (89kDa) by immunoblotting using cleared whole cell homogenates. Un-cleaved PARP served as a loading control (n=3). Percent PARP cleavage is shown in the right hand panel. * $P < 0.01$ *versus* untreated, † $P <$ at least 0.05 *versus* DOX+Z-FA-fmk. *E*, Caspase inhibition blunts DOX-mediated cardiomyocyte death. Cardiomyocytes treated as in *C*, but for 24 h, were analyzed for cell death by ELISA. * $P < 0.001$ *versus* untreated, † $P < 0.001$ *versus* DOX (n=12/group).

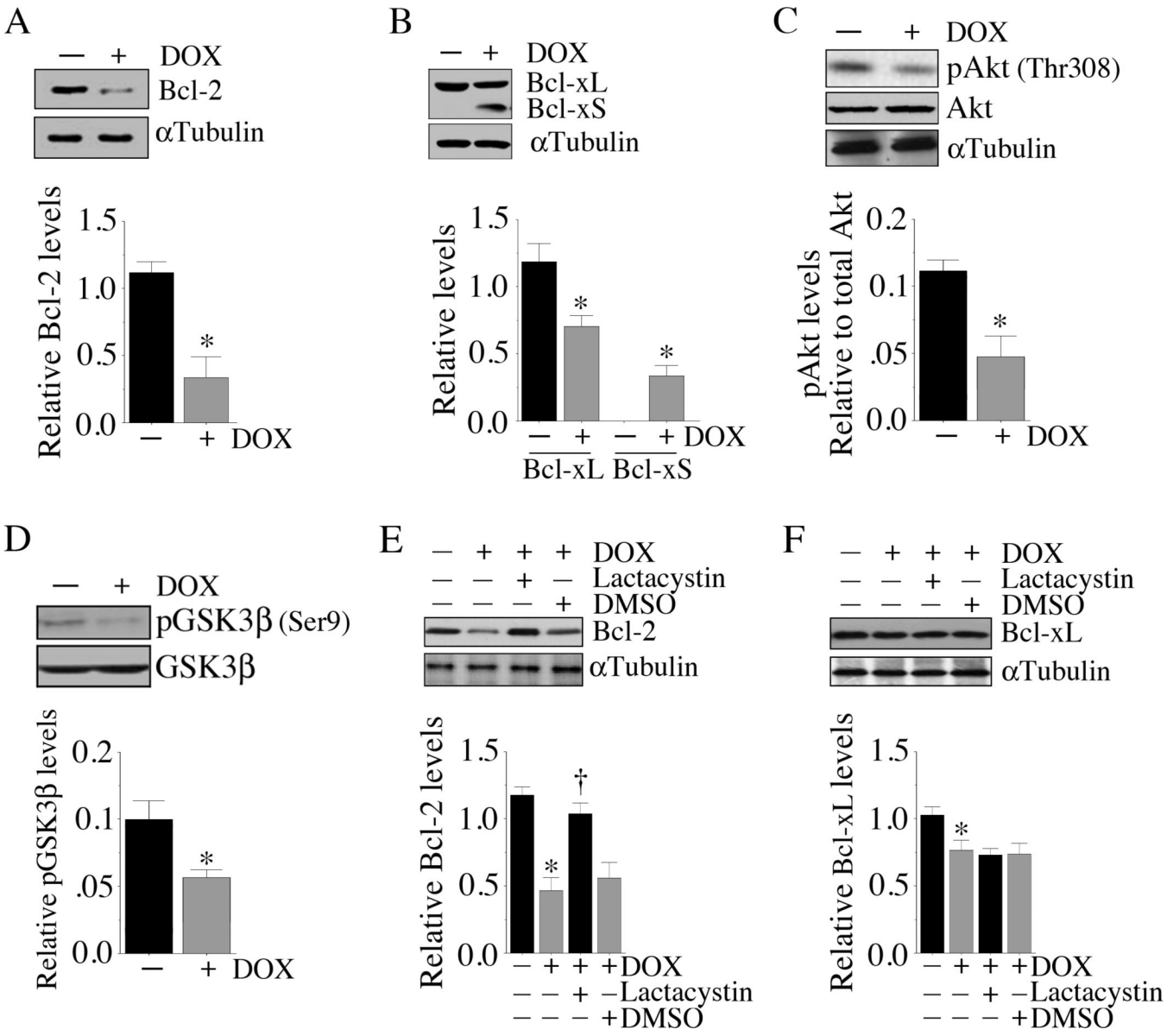

Fig. 4. DOX attenuates anti-apoptotic protein expression

A, DOX inhibits Bcl-2. Cardiomyocytes were treated DOX (1 μM for 6 h). Bcl-2 expression was analyzed by immunoblotting using cleared whole cell homogenates. αTubulin served as a loading control. Results from three 3 independent experiments are summarized in the lower panel. **P* < 0.01 *versus* untreated. *B*, DOX inhibits anti-apoptotic Bcl-xL, but induces pro-apoptotic Bcl-xS expression. Cardiomyocytes treated as in *A* were analyzed for Bcl-xL/xS expression by immunoblotting using cleared whole cell homogenates. αTubulin served as a loading control. Results from three 3 independent experiments are summarized in the lower panel. **P* < at least 0.05 *versus* untreated. *C*, DOX inhibit Akt activation. Cardiomyocytes treated as in *A*, but for an hour, were analyzed for pAkt (Thr308) levels by immunoblotting using cleared whole cell homogenates and activation-specific antibodies. Both total Akt and αTubulin served as loading controls. Results from three 3 independent experiments are summarized in the lower panel. **P* < 0.01 *versus* untreated. *D*, DOX inhibits pGSK3β levels. Cardiomyocytes treated as in *A*, but for two hours, were analyzed for total and pGSK3β (Ser9) levels by immunoblotting using cleared whole cell homogenates. Results from three 3

independent experiments are summarized in the lower panel. *$P < 0.05$ *versus* untreated. *E*, Proteasome inhibitor reverses DOX-induced Bcl-2 suppression. Cardiomyocytes were treated with the proteasomal inhibitor lactacystin (5 μM) for 30 min followed by the addition of DOX (1 μM for 6 h). Bcl-2 expression was then analyzed as in *A*. Results from three 3 independent experiments are summarized in the lower panel. *$P < 0.001$ *versus* untreated, †$P < 0.01$ *versus* DOX. *F*, Proteasome inhibitor fails to reverse DOX-induced Bcl-xL suppression. Cardiomyocytes treated as in *E* were analyzed for Bcl-xL expression by immunoblotting. Results from three 3 independent experiments are summarized in the lower panel *$P < 0.05$ *versus* untreated.

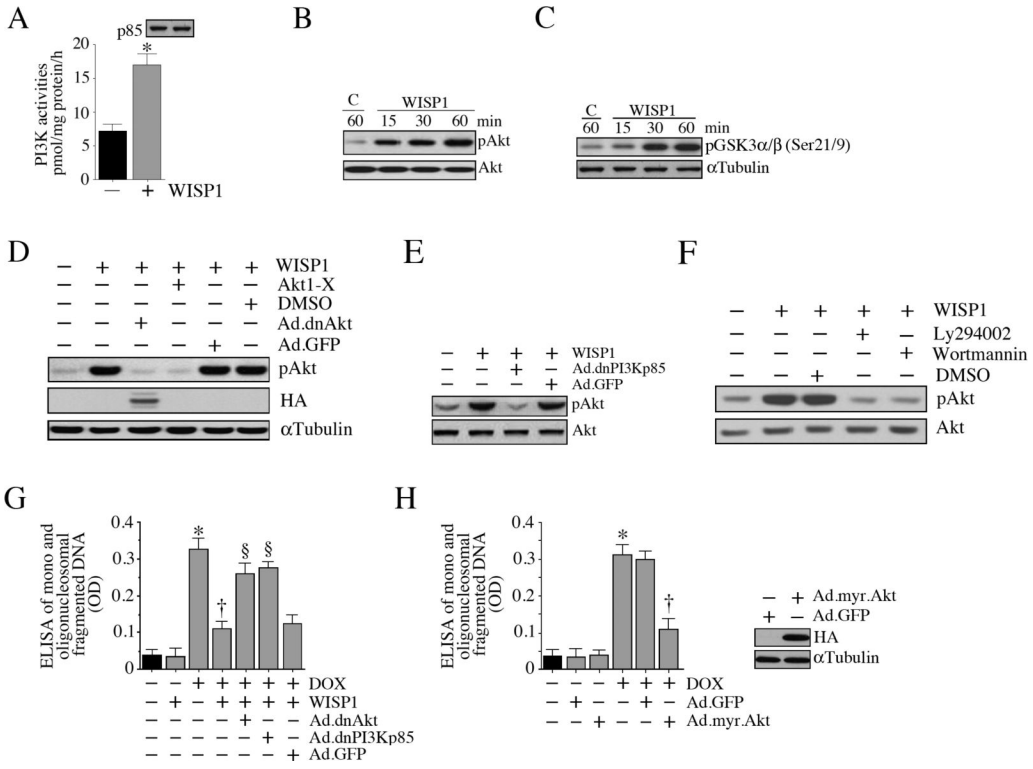

Fig. 5. WISP1 activates PI3K-Akt signaling

A, WISP1 induces PI3K activation. Cardiomyocytes were incubated with WISP1 (10 ng/ml for 1 h). p85α-associated PI3K activities were analyzed by ELISA as described in 'Materials and methods'. The *upper panel* shows immunoblot analysis of the same samples with anti-p85 antibody. * $P < 0.01$ *versus* untreated (n=6). *B*, WISP1 activates Akt. Cardiomyocytes treated as in *A* were analyzed for Akt activation by immunoblotting using cleared cell lysates and pAkt (Thr308) or Akt antibodies. A representative of three independent experiments is shown. *C*, WISP1 activates Akt kinase activity. Cardiomyocytes treated as in *A* were analyzed for Akt kinase activity using immunecomplex kinase assays. GSK3 served as a substrate (n=3). *D*, *E*, *F*, Pharmacological inhibitors of Akt and PI3K, and forced expression of dnAkt or dnPI3Kp85 by adenoviral gene transfer block WISP1 induced Akt activation. Cardiomyocytes were transduced (MOI 100 for 24 h) with Ad.dnAkt (D), or dnPI3Kp85 (E), or pretreated with Akt1-X (2.5 μM in water for 1 h; D), Ly294002 (25 μM in DMSO for 1 h; F) or wortmannin (250 nM in DMSO for 1 h; F) prior to WISP1 addition (10 ng/ml for 1 h). Ad.GFP and DMSO served as respective controls. Expression of HA was analyzed by immunoblotting (D; αTubulin served as a loading control). Total and pAkt (Thr308) levels were analyzed by immunoblotting (n=3). *G*. Forced expression of dnAkt and dnPI3Kp85 inhibit the pro-survival effects of WISP1. Cardiomyocytes treated as in *D and E* were analyzed for cell death at 24 h by ELISA. *$P < 0.001$ *v versus* untreated, †$P < 0.001$ *versus* DOX, §$P < 0.01$ *versus* DOX+WISP1 (n=12/group). *H*, Forced expression of constitutively active Akt inhibits DOX-mediated cell death. Cardiomyocytes were transduced with myr.Akt or GFP (MOI 100 for 24 h) prior to DOX addition (1 μM for 24 h). Cell death was analyzed by ELISA. *$P < 0.001$ *versus* untreated, †$P < 0.001$ *versus* DOX+Ad.GFP (n=12/group). Quantitation and significance of the data in panels B, C, D, E and F are presented in Supplementary Fig. S5.

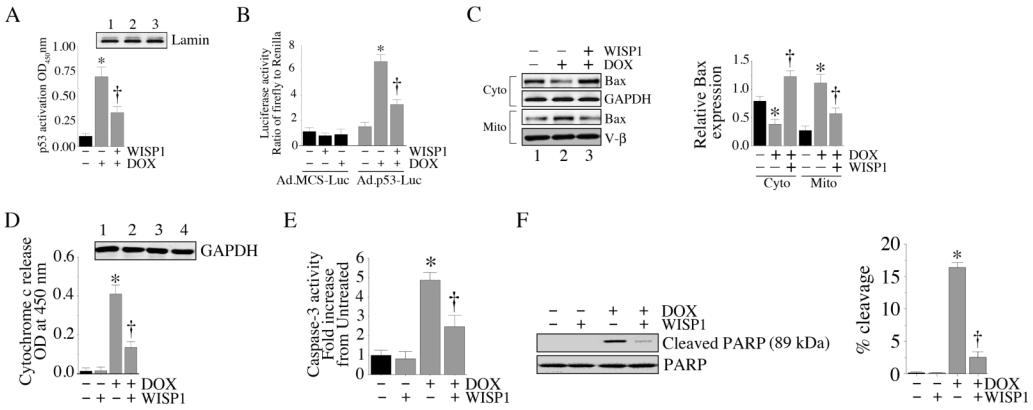

Fig. 6. WISP1 blocks DOX-stimulated pro-apoptotic signaling

A, WISP1 attenuates DOX-mediated p53 activation. Cardiomyocytes were incubated with WISP1 (10 ng/ml for 1 h) prior to DOX addition (1 μM for 3 h). Nuclear proteins were extracted and analyzed for p53 activation by ELISA. **P* < 0.001 *versus* untreated, †*P* < 0.01 *versus* DOX (n=3/group). *B*, WISP1 attenuates DOX stimulated p53-dependent reporter gene activity. Cardiomyocytes transduced with Ad-p53-Luc (MOI 50) were treated with WISP1 (10 ng/ml for 1h) followed by DOX (1 μM) for 7 h. Firefly and *Renilla* luciferase activities were then determined as described in 'Materials and methods'. * *P* < 0.001 *versus* untreated, †*P* < 0.01 *versus* DOX (n=12/group). *C*, WISP1 inhibits DOX-induced Bax mitochondrial translocation. Cardiomyocytes were treated with WISP1 (10 ng/ml for 1h) prior to DOX addition (1 μM for 8 h). Mitochondrial and cytoplasmic extracts were analyzed for Bax and cytochrome *c* levels by immunoblotting. Results from three independent experiments are summarized in the right hand panel. **P* < 0.05 *versus* respective untreated, †*P* < 0.01 *versus* respective DOX treatment. *D*, WISP1 attenuates DOX stimulated cytochrome *c* release. Cardiomyocytes were treated with WISP1 (10 ng/ml for 1 h) prior to DOX addition (1 μM for 8 h). Cytochome *c* levels in cytoplasmic extracts were analyzed by a colorimetric assay. Purity of cytoplasmic extracts and equal loading were confirmed by immunoblotting for GAPDH (inset). **P* < 0.001 *versus* untreated, †*P* < 0.001 *versus* DOX (n=6/group). *E*, WISP1 inhibits DOX-induced caspase-3 activation. Cardiomyocytes treated as in *D* were analyzed for Caspase-3 activation using a fluorescent method. **P* < 0.001 *versus* untreated, †*P* < 0.05 *versus* DOX (n=6/group). *F*, WISP1 inhibits DOX-mediated PARP activation. Cardiomyocytes treated as in *D* were analyzed for cleaved PARP (89kDa) by immunoblotting (n=3). Un-cleaved PARP served as a loading control. Percent PARP cleavage is shown in the right hand panel. **P* < 0.001 *versus* untreated, †*P* < 0.001 *versus* WISP1.

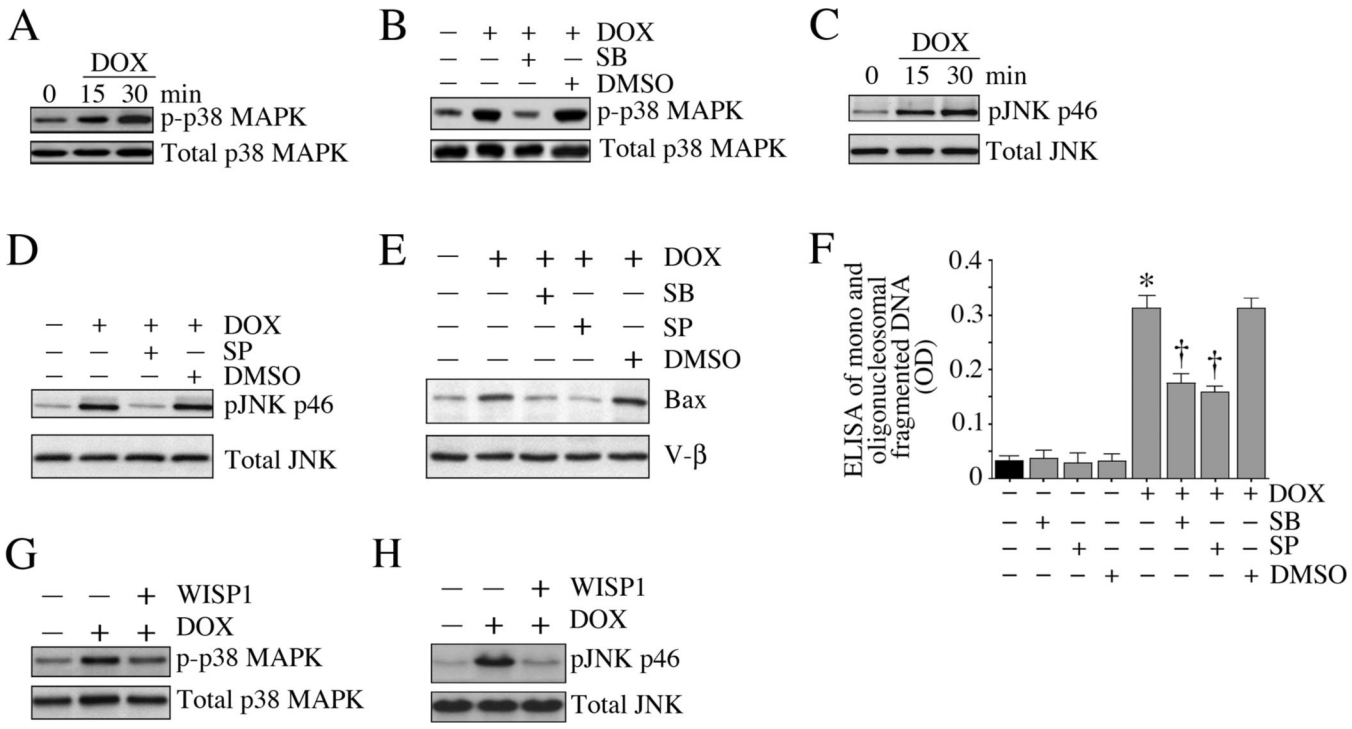

Fig. 7. WISP1 inhibits DOX-induced MAPK activation and cardiomyocyte death

A, DOX induces p38 MAPK activation. Cardiomyocytes were treated with DOX (1 μM) for the indicated time periods. p38 MAPK activation was analyzed by immunoblotting using activation-specific antibodies (p-p38 MAPK Thr180/Tyr182) and cleared whole cell homogenates (n=3). *B*, DOX-mediated p38 MAPK activation is inhibited by SB 203580. Cardiomyocytes were treated with SB 203580 (SB; 1 μM in DMSO for 30 min) prior to DOX (1 μM for 30 min) addition, and then analyzed as in *A* (n=3). *C*, DOX induces JNK activation. Cardiomyocytes treated as in *A* were analyzed for JNK activation by immunoblotting using activation-specific antibodies and cleared whole cell homogenates (n=3). *D*, SP 600125 inhibits DOX-mediated JNK activation (pJNK Thr183/Tyr185). Cardiomyocytes were treated with SP 600125 (SP; 20 μM in DMSO for 30 min) prior to DOX (1 μM for 30 min) treatment, and then analyzed as in *C* (n=3). *E*, SB and SP attenuate DOX-induced Bax translocation to mitochondria. Cardiomyocytes were treated with SB and SP prior to DOX addition (1 μM for 8 h). Bax levels in mitochondria were analyzed by immunoblotting. V-β served as a loading and purity control. *F*, SB and SP attenuate DOX-induced cardiomyocyte death. Cardiomyocytes were treated with SB and SP prior to DOX addition (1 μM for 24 h). Cell death was analyzed as in 1*A*. **P* < 0.001 *versus* untreated, †*P* < 0.001 *versus* DOX alone or DOX+DMSO (n=12). *G*, WISP1 inhibits DOX-mediated p38 MAPK activation. Cardiomyocytes were treated with WISP1 (10 ng/ml for 1 h) prior to DOX (1 μM for 30 min) addition, and then analyzed as in *A* (n=3). *H*, WISP1 inhibits DOX-mediated JNK activation. Cardiomyocytes were treated with WISP1 (10 ng/ml for 1 h) prior to DOX (1 μM for 30 min) addition, and then analyzed as in *C* (n=3). Quantitation and significance of the data in panels A, B, C, D, E, G and H are presented in Supplementary Fig. S7.

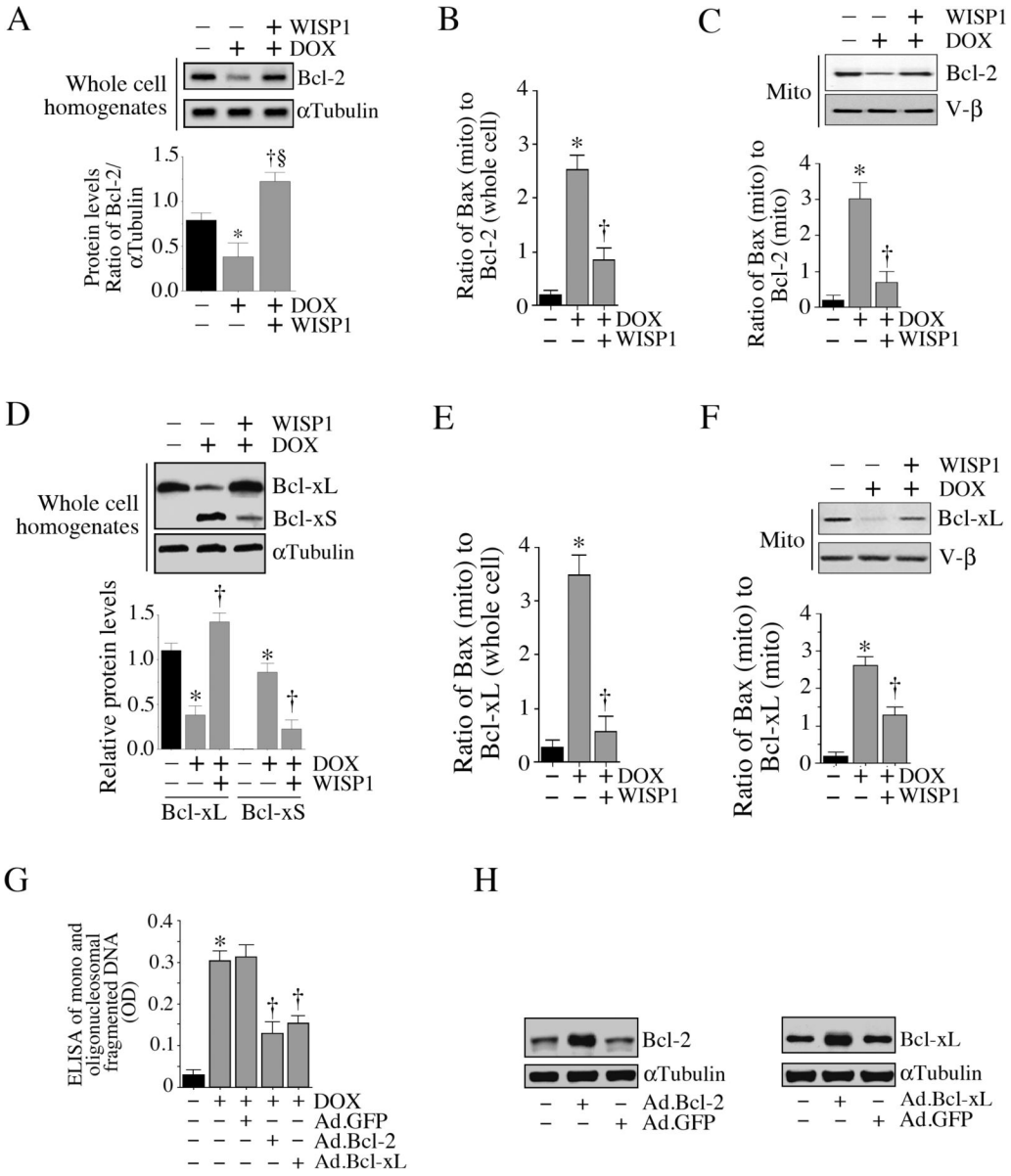

Fig. 8. WISP1 reverses DOX-induced Bcl2 and Bcl-xL repression

A, WISP1 reverses DOX-induced suppression of Bcl-2. Cardiomyocytes were treated with WISP1 (10 ng/ml for 1 h) prior to DOX addition (1 μM for 6 h). Bcl-2 expression was analyzed by immunoblotting. αTubulin served as a loading control. Results from three independent experiments are summarized in the lower panel. **P* < 0.05 *versus* untreated, †*P* < 0.05 *versus* untreated, §*P* < 0.01 *versus* DOX. *B*, WISP1 reduces Bax (mito) to Bcl-2 (total) ratio. Results from panel A (Bcl-2) and 6C (mito, Bax, lane 1) were plotted as a ratio of mitochondrial Bax levels to total (whole cell) Bcl-2 levels following DOX and DOX+WISP1 treatment. **P* < 0.001 *versus* untreated, †*P* < 0.01 *versus* DOX (n=3). *C*, WISP1 reverses DOX-induced suppression of Bcl-2 expression in mitochondrial fraction. Cardiomyocytes were treated as in *A*, but were analyzed for Bcl-2 levels immunoblotting using mitochondrial fraction. V-β served as a loading and purity control. Ratios of mitochondrial Bax to mitochondrial bcl-2 levels are shown in the lower panel. **P* < 0.001 *versus* untreated, †*P* < 0.01 *versus* DOX (n=3). *D*, WISP1 reverses DOX-induced suppression of Bcl-xL. Cardiomyocytes were treated with WISP1 (10

ng/ml for 1 h) prior to DOX addition (1 μM for 6 h). Bcl-x expression was analyzed by immunoblotting. αTubulin served as a loading control. Results from three independent experiments are summarized in the lower panel. **P* < 0.01 *versus* untreated, †*P* < at least 0.05 *versus* DOX, *E*, WISP1 reduces Bax (mito) to Bcl-xL (total) ratio. Results from panel *D* (Bcl-xL) and 6*C* (mito, Bax, lane 1) were plotted as a ratio of mitochondrial Bax levels to total (whole cell) Bcl-xL levels following DOX and DOX+WISP1 treatment. **P* < 0.001 *versus* untreated, †*P* < 0.001 *versus* DOX (n=3). *F*, WISP1 reverses DOX-induced suppression of Bcl-xL expression in mitochondrial fraction. Cardiomyocytes were treated as in *D*, but were analyzed for Bcl-2 levels immunoblotting using mitochondrial fraction. V-β served as a loading and purity control. Ratios of mitochondrial Bax to mitochondrial Bcl-xL levels are shown in the lower panel. **P* < 0.001 *versus* untreated, †*P* < 0.05 *versus* DOX (n=3). *G*, Forced expression of wild-type Bcl-2 or Bcl-xL inhibits DOX-induced cell death. Cardiomyocytes transfected with Ad.Bcl-2 or Ad.Bcl-xL (MOI 100 for 24 h; expression levels of Bcl-2 and Bcl-xL following transduction are shown in panel *H*, n=3) was treated with DOX (1 μM for 24 h). Cell death was analyzed by ELISA. **P* < 0.001 *versus* untreated, †*P* < at least 0.05 *versus* DOX+Ad.GFP (n=12/group).

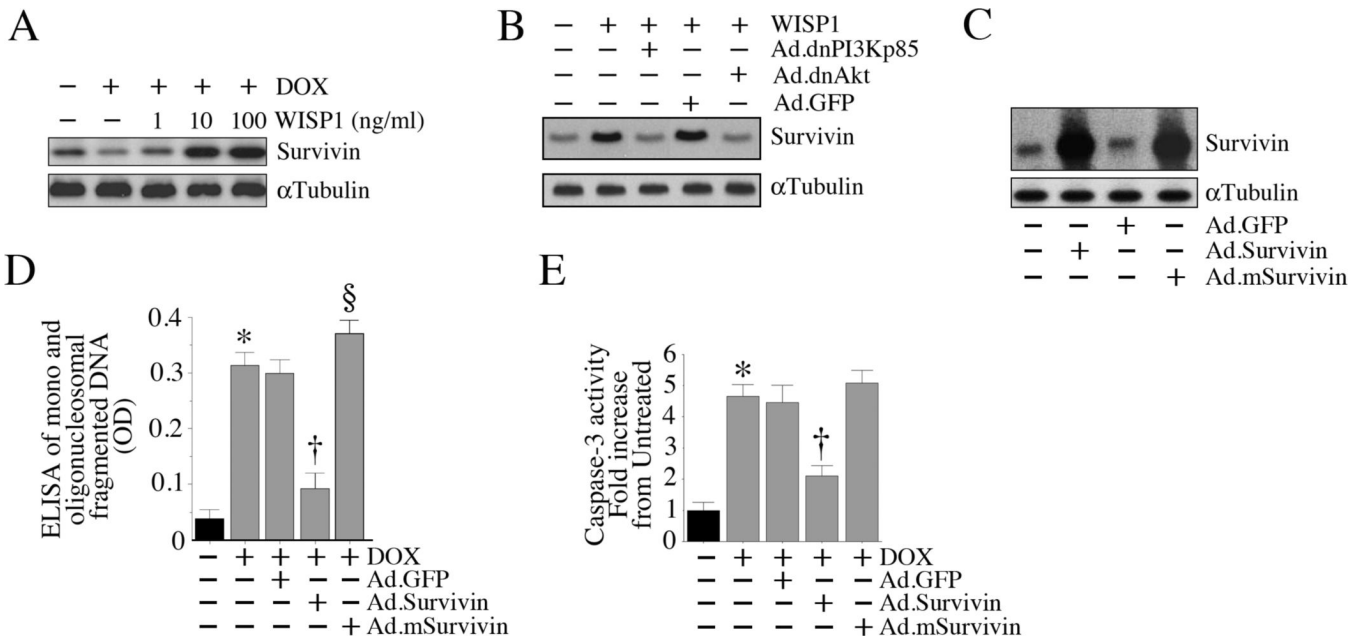

Fig. 9. WISP1 induces Survivin expression via PI3K-Akt signaling

A, WISP1 induces Survivin expression. Cardiomyocytes were treated with WISP1 (10 ng/ml) for 3 h. Cleared whole cell homogenates were then analyzed for Survivin protein levels by immunoblotting. αTubulin served as a loading control. A representative of three independent experiments is shown. *B*, WISP1 induces Survivin expression via PI3K and Akt. Cardiomyocytes transduced with dnPI3Kp85 or dnAkt were treated with WISP1 (10 ng/ml for 3 h). Survivin expression was analyzed by immunoblotting (n=3). *C*, Forced expression of Survivin blunts DOX-induced cell death. Cardiomyocytes were transduced with wild-type (Ad.Survivin) or mutant (Ad.mSurvivin) Survivin (MOI 100 for 24 h; overexpression of wild-type and mutant Survivin is confirmed by immunoblotting, n=3) prior to DOX addition (1 μM for 24 h). Cell death was analyzed by ELISA. **P* < 0.001 *versus* untreated, †*P* < 0.001 *versus* DOX, §*P* < 0.05 *versus* DOX (n=12/group).

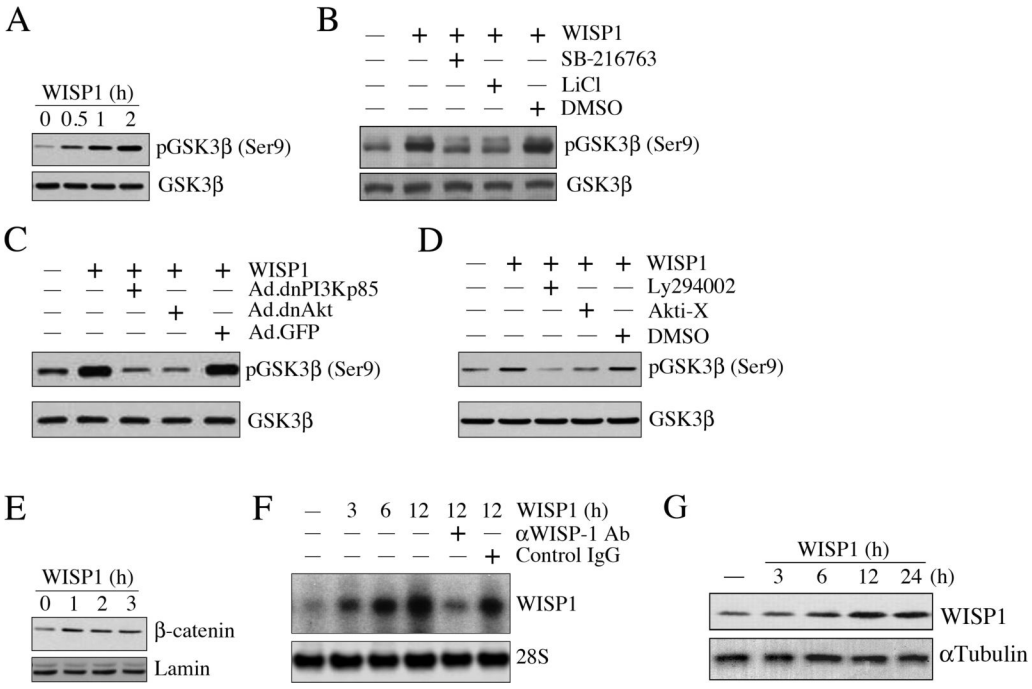

Fig. 10. WISP1 induces GSK3β phosphorylation, β-catenin translocation, and its own expression

A, WISP1 induces GSK3β phosphorylation. Cardiomyocytes were treated with WISP1 (10 ng/ml), and at the indicated time periods, whole cell homogenates were prepared and analyzed for total and phospho-GSK3β (Ser9) by immunoblotting (n=3). *B*, WISP1-mediated GSK3β phosphorylation is inhibited by SB-216763 and LiCl. Cardiomyocytes were treated with a GSK3β-specific inhibitor SB-216763 (1 nM in DMSO for 15 min) or LiCl (30 mM for 15 min) prior to the addition of WISP1 (10 ng/ml for 1h). Cleared whole cell homogenates were analyzed for total and phospho-GSK3β (Ser9) as in *A* (n=3). *C*, *D*, WISP1 induces GSK3β phosphorylation via PI3K and Akt. Cardiomyocytes were either transduced (*C*) with adenoviral vectors for dnPI3Kp85 and dnAkt (100 MOI for 24 h), or treated (*D*) with the PI3K inhibitor Ly294002 (25 μM in DMSO for 1 h) or Akt inhibitor Akti-X (2.5 μM in water for 1 h) prior to WISP1 addition (10 ng/ml for 1h). Cleared whole cell homogenates were analyzed for total and phospho-GSK3β (Ser9) as in *A* (n=3). *E*, WISP1 induces β-catenin nuclear translocation. Cardiomyocytes treated as in A were analyzed for β-catenin by immunoblotting using nuclear protein extracts (n=3). Lamin served as loading control. *F*, WISP1 induces its own expression. Cardiomyocytes were treated with WISP1 for the indicated time periods. Specificity of WISP1 was verified by incubating WISP1 (10 ng/ml) with neutralizing antibodies or control IgG (10 μg/ml for 1 h) before addition. WISP1 mRNA expression was analyzed by Northern blotting (n=3). 28S rRNA served as a loading control. *G*, WISP1 induces WISP1 protein expression. Cardiomyocytes treated as in *F* with WISP1, but for up to 24 h, were analyzed for WISP1 protein expression by immunoblotting using cleared whole cell homogenates (n=3). αTubulin served as a loading control. Quantitation and significance of the data in panels A-G are presented in Supplementary Fig. S10.

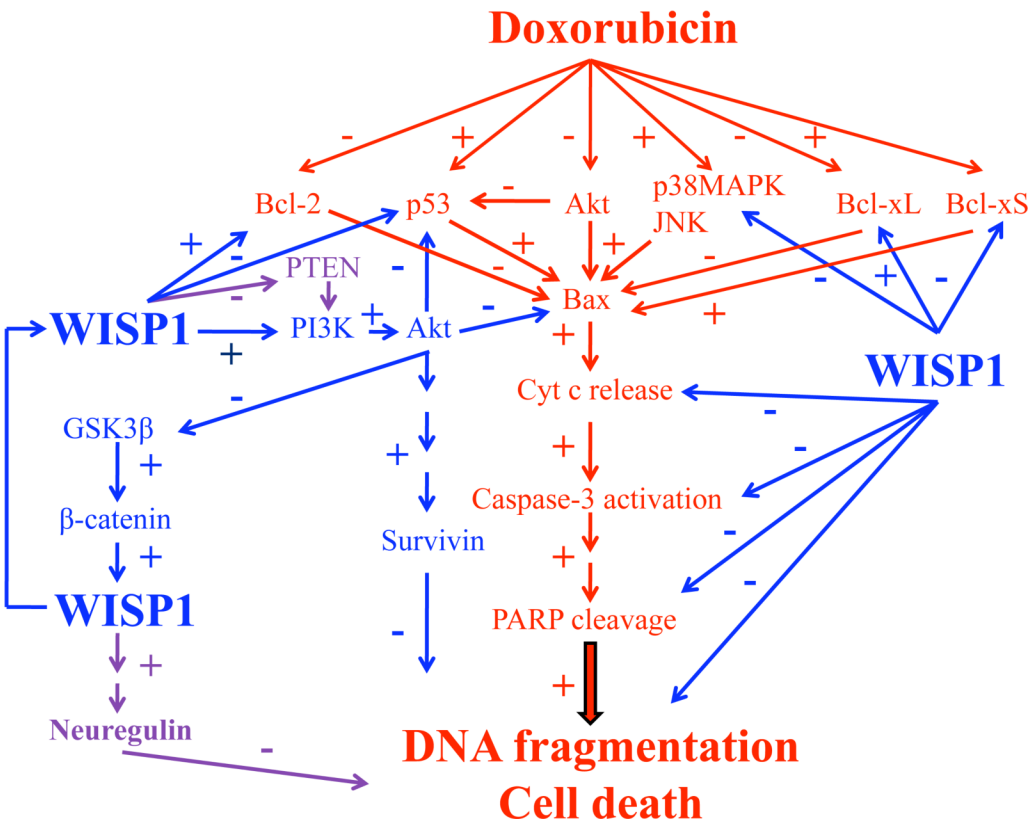

Fig. 11. Schema showing possible signal transduction pathways regulated by WISP1 in blocking DOX induced cardiomyocyte death

While the cell death pathways regulated by DOX are highlighted in red, the pro-survival effects of WISP1 are shown in blue. Few of the many signal transduction pathways that still needs investigation are highlighted in purple. The results here demonstrate that the CCN family member WNT1-Inducible Signaling Pathway Protein-1 (WISP1) can significantly inhibit doxorubicin (DOX)-induced cardiomyocyte death via activation of diverse cell survival pathways. WISP1 inhibits DOX-mediated p53 activation, p38MAPK and JNK phosphorylation, mitochondrial translocation of Bax, release of cytochrome c, activation of caspase-3, and suppression of Bcl-2 and Bcl-xL expression in cardiomyocytes. Further, WISP1 induces PI3K-dependent Akt activation, PI3K-Akt-dependent Survivin expression, GSK3β phosphorylation, β-catenin nuclear translocation, and its own induction.